Discovery of miRNA–RNA Biomarkers for Risk Stratification in Acute Myeloid Leukemia with Multi-Cohort Validation

Dona Hasini Gammune[1], Doan Bui[1], Tongjun Gu[1,2,3*]

[1]Versiti Blood Research Institute, Milwaukee, Wisconsin

[2]Data Science Institute, Medical College of Wisconsin, Milwaukee, Wisconsin

[3]Department of Biostatistics, University of Florida, Gainesville, Florida

*Corresponding author:

Tongjun Gu, PhD
Versiti Blood Research Institute
8727 W Watertown Plank Rd, Milwaukee, WI 53226
Email: tgu@versiti.org
Office: 414-937-3884

Abstract

Acute myeloid leukemia (AML) is a highly heterogeneous malignancy, and current prognostic standards such as the European LeukemiaNet (ELN) do not fully capture its underlying regulatory complexity. We developed a two-step, PCA-based survival workflow that independently and jointly analyzes gene and miRNA expression to identify biomarkers for patient risk stratification, followed by support vector machine (SVM) validation across multiple AML cohorts. This approach yielded a 19-gene panel—including known oncogenes (HMGA2, TAL1) and novel candidates (MLEC, APOE)—that achieved high validation accuracy relative to ELN (AUCs > 0.879). Parallel analyses identified a 16-miRNA panel enriched for tumor suppressors (miR-7b-3p, miR-26a-5p) and novel markers (miR-3613-5p, miR-942-5p). Integrating experimentally supported miRNA:gene interactions revealed 10 coherent regulatory pairs, most showing inverse correlations, improving performance over single-omic models. Finally, a Cox regression–based risk score accurately stratified patients and outperformed ELN. Overall, this framework provides biologically grounded biomarkers with strong prognostic power.

Statement of significance

This work introduces a multi-omic miRNA:gene framework that models regulatory programs at genome-wide scale and links miRNAs to their functional targets to generate mechanistically interpretable biomarkers. The resulting biomarkers provide a risk score that improves upon ELN-based stratification, offering a more precise and biologically informed foundation for clinical risk prediction and patient classification.

Introduction

Acute myeloid leukemia (AML) is an aggressive and heterogeneous hematologic malignancy, with 5-year overall survival rates remaining below 30% despite therapeutic advances (1). Prognostic stratification has been significantly improved by the European LeukemiaNet (ELN) 2017 and 2022 guidelines, which integrate cytogenetic and mutational features to guide therapy (2, 3). Nevertheless, substantial heterogeneity persists, as patients within the same ELN risk category often experience markedly different outcomes (2, 3), highlighting the need for additional biomarkers that capture broader molecular complexity and provide reproducible risk classification.

Gene expression and microRNAs (miRNAs) are key regulators of AML biology and prognosis, with growing evidence for their clinical relevance (4-6). Oncogenic drivers such as HMGA2 and CTGF, and tumor suppressors like GATA1, have demonstrated prognostic importance (7-13). Transcriptomic analyses have further identified genes including MME, RBM11, ENO1, and MYH9 as independent predictors of outcome (7). Concurrently, aberrant miRNA expression, such as elevated miR-155, miR-29b, miR-126, and miR-223, has been linked to adverse outcome, while miR-181 is consistently associated with favorable prognosis (5, 6, 14-18). Several miRNA-based therapeutics have already in clinical trials, underscoring their translational promise (19). Despite these advances, most studies have examined genes and miRNAs separately, neglecting their regulatory interplay. Given that miRNAs exert post-transcriptional control over RNAs, integrative analyses of miRNA:gene networks may yield biologically coherent signatures with enhanced prognostic power. Recent multi-omics approaches show that combining molecular layers can enhance predictive modeling beyond single-omic features (20, 21). Yet many potentially informative genes and miRNAs remain unexplored, particularly within regulatory networks that drive AML progression and treatment resistance.

In this study, we developed a PCA-based survival framework that simultaneously models genome-wide gene-expression and miRNA-expression profiles, enabling the capture of coordinated transcriptional and post-transcriptional programs. By incorporating experimentally validated miRNA:gene interactions, the framework yields an integrated set of regulatory features that supports mechanistic interpretation through identifiable regulatory axes. Gene and miRNA models were trained in The Cancer Genome Atlas Acute Myeloid Leukemia (TCGA-LAML) cohort and evaluated for gene-expression robustness in the Beat Acute Myeloid Leukemia Master Trial (BEATAML2.0), the Epigenomics Studies in Acute Myeloid Leukemia (ESAML) cohort, and the Genomics of Acute Myeloid Leukemia (GAML) cohort, with miRNA and miRNA:gene regulatory pairs independently validated in GAML. This approach identified a concise panel of genes, miRNAs, and miRNA:gene regulatory pairs with stronger prognostic value relative to ELN. These findings motivate the development of an expression-based molecular score that may serve as a practical complement to comprehensive cytogenetic classification schemas.

Results

Study populations

In the TCGA-LAML cohort, 200 patients were initially considered. ELN-2017 classifications were updated to ELN-2022 using cytogenetic and mutation information available in this cohort (See Methods; Supplementary Table S1). Based on ELN-2022, patients were assigned into three risk groups: Favorable (n = 81**)**, Intermediate (n = 37), and Adverse (n = 61) with 21 patients unclassifiable due to incomplete cytogenetic or molecular data (Supplementary Table S2A).

Self-reported race was dominated by WHITE (n = 150), followed by NH/C (n = 26) and BLACK (n = 10); other categories contained fewer than five individuals.

In the BEATAML2.0 cohort, 698 patients were initially available. 33 non-AML cases were removed, yielding 665 patients for analysis (Supplementary Table S3). ELN-2022 risk groups were derived analogously to TCGA-LAML: Favorable (n = 197), Intermediate (n = 103), and Adverse (n = 304) with 56 patients unclassified due to missing cytogenetic or molecular data (Supplementary Table S2B). To address incomplete ethnicity data in BEATAML2.0, a composite ethnicity variable was constructed as detailed in the Methods section. This approach yielded White (n = 360), AdmixedBlack (n = 10), HispNative (n = 26), Black (n = 15), Asian (n = 13), and smaller groups.

Among the 155 ESAML patients, ELN-2022 classifications were derived using criteria consistent with TCGA-LAML and BEATAML2.0, yielding 49 Favorable, 26 Intermediate, and 21 Adverse cases, while 59 patients were unclassifiable due to incomplete cytogenetic or molecular annotations (Supplementary Table S4; Supplementary Table S2C).

The GAML cohort included 43 patients. In the absence of ELN annotations, relevant analyses used Tumor versus Normal labels, including 17 Normal and 26 Tumor specimens.

Clinical characteristics and survival associations

Survival analyses confirmed the prognostic relevance of the ELN-2022 in TCGA-LAML (Fig. 1A–B). Median overall survival declined progressively from the Favorable to the Adverse group (Kruskal–Wallis $p = 0.00023$), and Kaplan–Meier curves demonstrated strong separation among the three risk groups (log-rank $p = 0.00032$). Age also differed significantly across ELN-2022 categories (Kruskal–Wallis $p = 0.0034$; Fig. 1C), with patients in the Adverse-risk group generally older. Consistently, age-stratified survival analysis (≤60 versus >60 years) revealed markedly shorter survival among older individuals (log-rank $p < 0.0001$; Fig. 1D). Corresponding analyses for the BEATAML2.0 are provided in Supplementary Fig. S1.

Age was significantly associated with survival in both TCGA-LAML and BEATAML2.0, whereas sex demonstrated prognostic relevance only in the BEATAML2.0 (Supplementary Fig. S1, S2 and S3). Ethnicity was not associated with survival in either cohort (Supplementary Fig. S2C-D and S3C-D). To account for demographic confounding, age and sex were included as covariates in all survival models. PCA of bulk gene-expression profiles demonstrated no clustering by age, sex, or race (Supplementary Fig. S4), indicating that demographic variables did not drive global transcriptional variation.

PCA-based multilevel framework for gene biomarker discovery

To systematically identify prognostic biomarkers, we developed a PCA-based multivariate survival-driven feature selection framework (Fig. 2). PCA was first applied to the TCGA-LAML expression matrix to reduce dimensionality while capturing major sources of biological variation. Unlike single-gene tests, this approach simultaneously evaluates the genome-wide expression landscape, allowing detection of gene–gene interactions and higher-order effects.

Principal components (PCs) explaining >50% cumulative variance were tested for association with overall survival using Cox models adjusted for age, sex, and ethnicity. Survival-associated PCs (BH-adjusted $p < 0.05$) were then used to identify top-contributing genes. The top 300 genes from each significant PC were subjected to a second PCA-based survival analysis within ELN-2022 categories to mitigate risk-group confounding. Genes consistently associated with survival in both TCGA-LAML and BEATAML2.0 were retained as robust candidates.

From this reproducible gene set, we applied SVM-based variable importance scoring (22) in the TCGA-LAML training cohort to prioritize the most informative prognostic genes. The resulting gene panel was validated across BEATAML2.0, ESAML, and GAML to ensure cross-cohort robustness. An identical pipeline was applied for miRNA discovery.

This multilevel strategy—combining PCA-based survival modeling, ELN-stratified refinement, cross-cohort reproducibility filtering, and SVM-based prioritization—enabled systematic identification of biologically meaningful and clinically relevant gene and miRNA biomarkers.

Identification of prognostic PCs and cross-cohort gene biomarkers

In TCGA-LAML, 20,098 genes were profiled, of which 14,265 met the count per million (CPM) > 1 thresholds (Details in Methods). PCA was performed to reduce dimensionality, retaining the top 20 PCs (cumulative variance > 50%) to capture both dominant and subtle biological variation across all genes simultaneously (Supplementary Fig. S5A).

Multivariant Cox models identified PC4 and PC5 as significantly associated with overall survival in TCGA-LAML (BH-adjusted $p < 0.05$; Supplementary Table S5). Notably, these PCs more effectively stratified patients by ELN risk groups than the top two PCs, underscoring their biological relevance (Supplementary Fig. S5B). For each survival associated PC, the 300 genes with the largest absolute loadings were selected for a second round of PCA-based, ELN-stratified survival analysis, yielding 397 candidate genes in TCGA-LAML. In the BEATAML2.0 cohort, Cox analysis identified PC5, PC7, and PC11 as survival associated (Supplementary Table S5). Applying the same loading-based selection procedure yielded 698 survival-related genes (Supplementary Fig. S6).

Cross-cohort comparison identified 77 genes common across ELN risk groups, of which 35 showed consistent hazard ratio (HR) patterns in both cohorts (Supplementary Fig. S7, Supplementary Table S6). These 35 genes included known AML-associated markers as well as previously unreported candidates**,** highlighting a mix of validated biomarkers and new potential prognostic markers.

Predictive power of established and novel genes for AML risk classification

We next evaluated the ability of known AML genes, novel candidate genes, and their combinations to classify patients into Favorable and Adverse ELN risk groups using SVM models (Fig. 3). SVM classifiers were trained in the TCGA-LAML cohort and validated across three independent cohorts: BEATAML2.0, ESAML, and GAML. According to Döhner et al. (2022) (3), the ELN-2022 Intermediate category includes patients with cytogenetic and/or molecular abnormalities that do not meet criteria for either Favorable or Adverse risk, resulting in a biologically heterogeneous and clinically ambiguous group. Therefore, we restricted downstream analyses to the Favorable and Adverse groups to ensure clearer biological interpretation and minimize misclassification bias.

Both established AML-associated genes and newly identified candidates demonstrated strong and reproducible discrimination across independent cohorts (Fig. 3A). In the TCGA-LAML training cohort, known genes achieved an AUC of 0.906, while novel candidates reached 0.914, and their combination yielded an AUC of 0.916. Validation in the independent BEATAML2.0 cohort showed similarly robust performance: known genes achieved an AUC of 0.851, novel genes 0.862, and the combined panel 0.876, demonstrating cross-cohort generalizability. ESAML exhibited excellent reproducibility despite platform and cohort differences, with AUCs of 0.852 (known), 0.859 (novel), and 0.895 (combined). Although GAML contains Tumor versus Normal rather than ELN categories, the TCGA-trained model still achieved clear biological separation (AUCs: 0.812, 0.820, and 0.845), indicating that these gene sets capture core AML biology rather than cohort-specific patterns.

Complementary performance metrics (Fig. 3B), including precision (0.82–0.91), recall (0.80–0.89), F1 score (0.81–0.90), specificity (0.83–0.92), and accuracy (0.82–0.90), were consistent across all cohorts, further highlighting the robustness and cross-cohort transferability of the TCGA-derived model and the compact gene feature set.

To identify the most prognostic gene features in AML, we ranked all known and novel genes in TCGA-LAML using SVM-based importance scoring (Supplementary Table S7). Genes with an importance score > 30 were designated as highly predictive, yielding a refined 19-gene panel composed of both well-established AML drivers and previously unrecognized novel biomarkers (Supplementary Table S8, Fig. 3E and Supplementary Fig. S8). Notably, several novel genes surpassed canonical AML genes in importance, highlighting their potential biological and clinical relevance.

We then trained an SVM classifier using this 19-gene panel exclusively in TCGA-LAML and validated in BEATAML2.0, ESAML, and GAML (Fig. 3A). The model achieved an AUC of 0.922 in TCGA-LAML and maintained strong performance in BEATAML2.0 (AUC = 0.905) and ESAML (AUC = 0.908). In GAML, the panel continued to produce clear biological separation (AUC = 0.879). Complementary evaluation metrics showed similarly robust performance across all cohorts (Fig. 3B). Together, these results confirm the reproducibility and cross-cohort generalizability of the 19-gene panel in diverse AML populations.

To further assess the robustness of our gene signatures, we performed a reversal analysis in which SVM models were trained in BEATAML2.0 and validated in TCGA-LAML (Fig. 3C). The BEATAML2.0-trained classifier demonstrated strong discrimination in TCGA-LAML (AUCs of 0.866–0.909 across gene sets), and evaluation metrics remained consistently high in both directions (Fig. 3D), reinforcing the stability of the gene panel across independent cohorts.

To confirm that the model performance reflected genuine biological signal rather than chance or overfitting, we conducted a negative-control analysis using 100 randomly selected 35-gene sets that were not associated with survival in any cohort. As expected, these models performed poorly (mean AUC = 0.600 in TCGA-LAML; 0.595 in BEATAML2.0; accuracies = 0.45 and 0.44; Supplementary Fig. S9), confirming that the predictive strength of the 19-gene panel derives from meaningful biological and clinical associations rather than random variation.

Gene set enrichment analysis revealed that the 19-gene panel was significantly enriched for functions related to basophil and mesodermal cell differentiation, response to other organism/biotic stimulus, and negative regulation of double-strand break repair (Supplementary Table S9), highlighting core mechanisms of AML pathogenesis. Basophil-differentiation factors

(TAL1, GATA1) are key regulators of myeloid lineage specification and leukemogenesis, and their dysregulation is consistent with the differentiation blockade characteristic of AML (23). Enrichment of biotic-stimulus and organism-response pathways points to broad perturbation of immune and inflammatory signaling, which is increasingly recognized as a driver of leukemic blast survival, immune tolerance, and immune evasion (24). Mesodermal cell–differentiation genes suggest reactivation of primitive developmental and stemness-associated programs that are frequently observed in high-risk, stemness-enriched AML states (25). Finally, the inclusion of HMGA2, C1QBP, and OTUB1, which modulate double-strand break repair and broader DNA damage responses, supports a model of impaired genomic maintenance and increased genomic instability (26). Collectively, these enriched processes encompass differentiation arrest, immune–inflammatory activation, primitive developmental reprogramming, and defective DNA repair—hallmark features of aggressive AML.

Identification of prognostic PCs and cross-cohort miRNA biomarkers

Using the same PCA-based survival workflow applied to gene expression, analysis of miRNA expression in TCGA-LAML identified 362 miRNAs significantly associated with overall survival (BH-adjusted $p < 0.05$; Supplementary Table S10). ELN-stratified PCA further refined this set to 202 miRNAs showing risk-specific expression patterns. In GAML, 77 miRNAs were differentially expressed between Tumor and Normal samples (BH-adjusted $p < 0.05$; Supplementary Table S11), of which 32 overlapped with TCGA-LAML, representing candidates with both prognostic and diagnostic relevance (Supplementary Fig. S10).

PCA of miRNA expression in TCGA-LAML revealed distinct separation patterns, with PC1 and PC5 emerging as significant components that more effectively discriminated ELN risk groups than the top two PCs (Supplementary Fig. S11A-B). Similarly, the significant miRNAs identified in GAML clearly separated Tumor from Normal samples and outperformed the first two PCs derived from the full miRNA expression set (Supplementary Fig. S11C-D) underscoring the strong stratification capacity of the selected miRNAs.

Predictive power of established and novel miRNAs in ELN risk and tumor classification

We next evaluated the predictive utility of miRNAs for AML risk stratification using the same SVM workflow applied to gene-based modeling. Models were trained in TCGA-LAML using known AML-associated miRNAs, novel candidates, and their combined set (Fig. 4A). All three sets showed strong discrimination between Favorable and Adverse groups, with training accuracies of 0.84–0.90 and AUCs of 0.918–0.927 (Fig. 4B). miRNAs were then ranked by SVM importance, and the top 16 features (importance > 30; Supplementary Table S12) were selected as a refined panel. The 16-miRNA panel performed best in training, achieving 0.92 accuracy, 0.93 precision, 0.88 recall, 0.94 specificity, and an AUC of 0.933.

Validation in the independent GAML cohort confirmed robust generalizability across cohorts. All miRNA sets achieved high performance, with the 16-miRNA panel again showing the best performance, with 0.86 accuracy, 0.89 precision, 0.89 recall, and an AUC of 0.916 (Fig. 4A-B). These results indicate that the selected miRNAs capture robust AML-related expression patterns across cohorts.

The final 16-miRNA biomarker panel (Fig. 4C; Supplementary Fig. S12; Supplementary Table S13) contained both established AML-associated miRNAs and high-ranking novel candidates. Interestingly, most known AML associated miRNAs (8 of 10) were tumor repressors, whereas

most known AML associated genes (7 of 8) were oncogenes (Supplementary Table S8, S13; fisher exact test p = 0.015), suggesting the complementary role of tumor-suppressive miRNAs and oncogenic RNAs in AML risk stratification.

miRNA:gene regulatory interactions in AML

To explore potential post-transcriptional regulation, we examined expression correlations between significant miRNAs and their target genes obtained from TarBase-v9.0 (27), an experimentally validated miRNA:gene interaction database (Details are in Methods; Supplementary Table S14). Spearman correlation analysis identified multiple significant associations (p value < 0.05; Supplementary Table S15). The top interactions—selected based on statistical significance ($p < 0.05$) and effect size ($\rho \geq 0.10$ or $\rho \leq -0.10$)—were summarized in Table 1.

Table 1. Significant correlations between top-ranked miRNA:gene pairs in TCGA-LAML.

Gene	miRNA	Spearman Correlation (ρ)	p- value
FHL2*	miR-32-5p	-0.32	0.001
HMGA2*	miR-32-5p	-0.16	0.024
MDH2*	miR-942-5p	-0.16	0.047
APOE	miR-32-5p	-0.10	0.025
MLEC	miR-3613-5p	-0.20	0.011
CCDC57	miR-26a-5p*	-0.15	0.046
DEPDC7	miR-942-5p	0.16	0.006
FHL2*	miR-3613-5p	0.14	0.014
IRF8	miR-1260a	0.31	0.000
MLEC	miR-181a-3p*	-0.27	0.000

* Indicates the known AML associated genes and miRNAs.

Several miRNA:gene pairs displayed inverse associations consistent with canonical miRNA-mediated repression. For example, the miR-181a-3p:MLEC pair showed a significant negative correlation ($\rho = -0.27$, $p < 0.001$), with miR-181a-3p expression increasing and MLEC expression decreasing from Favorable to Adverse ELN-2022 groups (Fig. 5A). A similar inverse pattern was observed for miR-942-5p:MDH2 ($\rho = -0.16$, $p = 0.047$; Supplementary Fig. S13). Additional inverse relationships included miR-32-5p:FHL2, miR-26a-5p:CCDC57, and miR-32-5p:HMGA2, each involving target genes such as FHL2 (9, 10), HMGA2 (7, 8, 26), and MDH2 (28), that are well-established AML-associated genes, supporting the biological plausibility of these interactions (Table 1).

In contrast, three miRNA:gene pairs showed positive correlations. miR-3613-5p:FHL2 ($\rho = 0.14$, $p < 0.014$; Fig. 5B), miR-1260a:IRF8 ($\rho = 0.31$, $p < 0.001$), and miR-942-5p:DEPDC7 ($\rho = 0.16$, $p = 0.006$) (Table 1; Supplementary Fig. S13). These positive associations may reflect shared upstream regulation, indirect signaling relationships, or feedback mechanisms, indicating that

AML-related post-transcriptional regulation extends beyond simple repression. Together, these findings show that both canonical and non-canonical interactions contribute to the miRNA:gene regulatory landscape underlying AML pathogenesis.

Integrated predictive modeling of miRNA:gene pairs

To determine whether integrating miRNA:gene interactions improve risk prediction, we trained SVM classifiers in TCGA-LAML using three feature sets: genes only, miRNAs only, and combined miRNA:gene pairs. The trained models were validated in the independent GAML cohort (Fig. 5C–D). In TCGA-LAML, AUCs were 0.900 for genes, 0.917 for miRNAs, and 0.923 for the combined set. Validation in GAML yielded similarly high AUCs—0.875, 0.898, and 0.903, respectively. Across both cohorts, the combined model performed best, indicating that integrating miRNAs with their target genes captures complementary, non-redundant biological information relevant to AML risk.

In TCGA-LAML, the combined classifier achieved an accuracy of 0.92, precision of 0.91, recall of 0.91, F1 of 0.91, and specificity of 0.93, outperforming either genes or miRNAs alone. A similar pattern held in GAML, where the combined model reached an accuracy of 0.89 with balanced precision and recall (0.88 each). PCA of the ten selected miRNA:gene pairs further separated Favorable and Adverse groups (Supplementary Fig. S14A), and feature importance rankings for the combined panel are summarized in Supplementary Table S16.

Cox regression-based integrated risk score improves prognostic stratification beyond ELN-2022

To develop a clinically actionable stratification tool, we constructed a Cox regression–based risk score using the ten selected miRNA:gene pairs (Fig. 6D). Using the cohort median (0.021; IQR: –0.430 to 0.435) as the cutoff, patients with scores ≥ 0.021 were classified as High risk and those below as Low risk. Cross-validated and full-model predictions showed clear separation across ELN categories, with higher scores consistently observed in Adverse-risk patients (Supplementary Fig. S14B). The resulting Low versus High groups demonstrated a marked and highly significant difference in overall survival ($p < 0.0001$; Fig. 6A), confirming strong prognostic discrimination within TCGA-LAML cohort.

Next, we compared the classifications by this risk score with ELN-2022. As shown in Fig. 6B–C, the molecular score produced meaningful reclassifications relative to ELN. Although six ELN-Favorable patients were reclassified as High risk, their survival closely resembled that of the ELN-Adverse group. Conversely, the two ELN-Adverse patients reassigned to the Low-risk group demonstrated markedly longer survival than ELN-Favorable group. These shifts aligned more closely with observed survival outcomes (Fig. 6B), indicating that the integrated molecular score provides more accurate prognostic stratification than ELN-2022 alone.

To formally quantify prognostic improvement, we compared five Cox proportional hazards models (Models 1–5; Detailed in Methods) in TCGA-LAML and independently validated the results in BEATAML2.0 (Supplementary Fig. S15; Supplementary Tables S17–S18). Compared with the ELN-only model (Model 1), adding the continuous molecular risk score (Model 2) markedly improved performance, reducing Akaike Information Criterion (AIC) from 925.08 to 885.50 ($\Delta AIC = 39.58$). As decreases in AIC > 10 provide strong evidence favoring the superior model (29), this result demonstrates that the integrated molecular score adds significant prognostic value beyond ELN-2022.

To directly compare categorical classifications, we dichotomized the continuous risk score at the threshold of 0.021 to define High and Low molecular-risk groups and evaluated two parallel models using only Favorable and Adverse patients: the ELN-based model (Model 3A) and the molecular risk–based model (Model 3B). Replacing ELN categories with molecular risk groups reduced the AIC from 499.24 to 488.36 (ΔAIC = 10.88). In Model 3B, Low molecular-risk status showed a highly significant protective effect (β coefficient = −1.45; BH-adjusted $p = 8.72 \times 10^{-}$□), corresponding to a hazard ratio lower than 1, indicating substantially reduced risk. This demonstrates that the molecular classifier provides markedly improved stratification of patients according to survival outcomes.

We further assessed whether combined molecular features from the ten miRNA:gene pairs enhanced prognostic modeling. Cox models incorporating both genes and miRNAs alongside ELN (Model 4A) or without ELN (Model 4B) outperformed the ELN-only baseline (AIC=925.08), yielding AIC values of 914.68 (Model 4A) and 489.22 (Model 4B). Gene-only models showed similar improvement: Model 5A (with ELN) achieved an AIC of 914.79, and Model 5B (without ELN) achieved 487.61. These findings confirm that these biomarkers retain strong independent prognostic relevance on their own and can surpass the predictive performance of ELN-2022 both as complementary features and as independent predictors.

Analyses were independently replicated in the BEATAML2.0 cohort using gene markers, where molecular biomarker-based models again outperformed ELN-only models (Supplementary Table S18), confirming the robustness and cross-cohort generalizability of the molecular risk score. Collectively, these results demonstrate that the ten miRNA:gene biomarkers and the derived risk score provide consistently superior prognostic information compared with ELN-2022 and represent a powerful refinement to current AML risk-stratification frameworks.

Discussion

In this study, we developed a PCA–based survival framework coupled with SVM validation to identify biomarkers with strong prognostic power and translational relevance. Unlike the common approaches of analyzing each gene individually, such as differential expression analysis, our framework evaluates all genes and miRNAs simultaneously, capturing higher-order regulatory patterns that more accurately reflect AML biology. Using this strategy, we derived a 19-gene panel and a 16-miRNA panel that achieved high accuracy in ELN risk classification. Incorporation of experimentally validated miRNA:gene interactions further revealed mechanistically coherent signatures linking oncogenic drivers with tumor-suppressive miRNAs, yielding ten regulatory pairs that consistently outperformed single-omic models. To translate these biomarkers into a clinically applicable metric, we constructed a Cox regression–based risk scores whose stable coefficients and cohort-median cutoff (0.021) provided a practical basis for patient stratification. Model-comparison analyses showed that adding this molecular score substantially improved survival prediction beyond ELN-2022, yielding large reductions in AIC and clear independent prognostic value. This compact, reproducible, and biologically interpretable signature offers immediate potential for refined clinical risk assessment and personalized therapeutic decision-making.

Accurate risk-group assignment is critical for evaluating prognostic biomarkers. We therefore harmonized ELN-2022 classifications across the TCGA-LAML, BEATAML2.0, and ESAML using the updated criteria of Döhner *et al*. (2022) (3), which incorporates revised cytogenetic abnormalities and expanded mutational categories, representing a substantial improvement over publicly available ELN-2017 annotation. To ensure consistent assignment, we applied a

reproducible rule-based classifier that integrates cytogenetic, structural-variant, and mutation data. Cohort-specific classifications are provided in Supplementary Tables S1, S3, and S4, with full workflow details described in the Supplementary Methods.

This study introduces several methodological and translational advances. Our framework moves beyond conventional one-gene-at-a-time testing by jointly modeling genome-wide expression, thereby capturing gene–gene dependencies and higher-order interactions that traditional approaches overlook. Unlike prior studies that analyze mRNAs or miRNAs in isolation (30, 31, 32), our integrated miRNA:target architecture leverages validated regulatory relationships and provides superior predictive performance. Linking miRNAs with their targets also enhances biological interpretability by revealing regulatory axes with potential therapeutic relevance. The resulting expression-based biomarkers are practical for clinical implementation and complement existing comprehensive cytogenetic and mutation classifiers. Finally, the derived molecular risk score meaningfully reclassifies patients—particularly those in Intermediate ELN groups—highlighting its potential to refine AML risk stratification and support more precise treatment decisions.

Consistent with prior studies, established oncogenes, such as HMGA2, CTGF, TAL1, and FHL2, emerged as strong predictors of adverse outcomes (AUC = 0.906) (7-11, 23, 26), reaffirming their central role in leukemogenesis. Importantly, we identified novel candidates, including MRPL16, CCDC57, NAGLU, and MLEC, that have not been previously implicated in AML prognosis yet demonstrated comparable or superior classification performance (AUC = 0.914). Notably, integrative models combining top known and novel genes achieved the highest performance (AUC = 0.922), underscoring that incorporating under-recognized features enhances classification accuracy (Fig.3A). These findings extend current knowledge by introducing new biomarkers that may refine ELN classification (2, 3), which often fails to fully capture the molecular heterogeneity of AML (1). The observed incremental gains achieved here suggest that additional undiscovered biomarkers remain, and that continued exploration of under-characterized genomic features could further improve AML stratification. Notably, our gene panel outperformed previously published models (AUCs: 0.78 in Ng et al., (2016); (30) 0.72 in Lai et al., (2022) (31)), demonstrating clear improvements in predictive power.

Our analysis also revealed both established and novel miRNAs with significant prognostic and diagnostic value. Well-established miRNAs, including miR-26a-5p, previously associated with favorable outcomes in AML (18, 33, 34), retained high predictive accuracy across cohorts (AUC = 0.918). Novel candidates, such as miR-3613-5p and miR-942-5p, consistently stratified patients (AUC = 0.923), highlighting their potential as unrecognized regulators of leukemic biology. Integrating established and novel miRNAs further improved predictive accuracy (AUC = 0.933), demonstrating that miRNA features capture unique biological processes not reflected in gene expression alone (Fig. 4A). Notably, our miRNA panel outperformed earlier models (AUC <0.70 in Ellson et al., (2024) (32)), demonstrating a marked gain in predictive power.

Our analyses highlight the complexity of miRNA:gene regulatory dynamics in AML. While several pairs exhibited canonical repression, three showed non-canonical positive correlations, likely reflecting indirect effects or shared upstream transcriptional programs. These findings indicate that miRNA:gene relationships in AML encompass both classical repression and alternative co-regulatory mechanisms that merit further investigation.

A representative canonical example is the miR-181a-3p:MLEC pair, which exhibits classical repression, with a significant negative correlation ($\rho = -0.27$, $p < 0.001$) and opposing

expression shifts from Favorable to Adverse ELN-2022 groups (Fig. 5A). MLEC encodes malectin, an endoplasmic reticulum (ER) lectin involved in glycoprotein folding and ER-stress responses (35, 36,). Although MLEC has not been directly linked to AML, it has been reported to exert a protective effect and serve as a prognostic marker in gastric cancer (37), suggesting context-dependent roles in tumor biology. miR-181a-3p, in contrast, has well-established functions in hematopoiesis and AML pathogenesis. It regulates myeloid differentiation, modulates apoptosis, and has been repeatedly associated with treatment response and prognosis in AML (38, 39). In our analysis, miR-181a-3p and MLEC not only showed strong inverse correlation but also displayed opposite hazard ratios in survival modeling, further supporting a functional regulatory relationship. Together, these patterns highlight a novel and biologically plausible miRNA:target axis that may contribute to AML risk stratification and warrants further mechanistic exploration.

In contrast, the miR-3613-5p:FHL2 pair demonstrates non-canonical co-regulation, with both features upregulated in higher-risk categories (Fig. 5B). FHL2 promotes leukemic proliferation while miR-3613-5p acts as an oncogenic microRNA in lung adenocarcinoma (40), gastric cancer (41), and breast cancer (42), driving proliferation, migration, EMT, and chemoresistance. Although miR-3613-5p has not been studied in AML, its elevated expression in Adverse-risk groups parallels its behavior in solid tumors. The concordant increases in miR-3613-5p and FHL2 therefore suggest shared upstream activation rather than classical miRNA-mediated repression.

Interestingly, STRING database (v12.0) (43) analysis revealed no direct protein-protein interactions among the eight genes forming the 10 miRNA:gene pairs (Supplementary Fig. S16), yet several miRNAs targeted multiple genes (Table 1). For example, miR-32-5p negatively correlated with FHL2, HMGA2, and APOE, suggesting that miRNAs may act as the primary connectors within these regulatory networks. FHL2 and HMGA2 are well-established AML oncogenes with upregulated expression in Adverse compared to Favorable: FHL2, a LIM-domain transcriptional co-regulator, interacts with β-catenin to activate oncogenic signaling and drive hematopoietic proliferation (44), and has been implicated in AML progression and poor prognosis (9, 10, 45). HMGA2 has also been strongly linked to leukemogenesis. Elevated HMGA2 has been shown to enhance self-renewal capacity of leukemic stem cells, thereby sustaining disease progression (7, 8, 26). In contrast, APOE, a lipid transport protein extensively studied in Alzheimer's disease and cardiovascular disorders, remains largely unexplored in AML (46, 47). Although no direct interactions among FHL2, HMGA2, and APOE have been established, its progressive upregulation from favorable to adverse groups, coupled with shared regulation by miR-32-5p, suggests a potential oncogenic role that warrants further investigation.

Our study has several limitations that also point to future directions. First, rigorous experimental validation of the discovered miRNA:gene regulatory pairs, particularly the positively correlated interactions, is needed to confirm their biological causality. Second, expanding this framework to integrate additional molecular layers, such as DNA methylation and RNA editing, could provide a more comprehensive systems-level understanding of AML biology. Finally, complementary integration with established genetic and cytogenetic markers could further refine risk stratification and support more personalized therapeutic decision-making.

Methods

Study cohorts and data acquisition

Transcriptomic and small RNA expression data were obtained from four independent AML cohorts. Gene expression profiles were analyzed from TCGA-LAML (dbGaP accession: phs000178; GDC Project ID: TCGA-LAML), BEATAML2.0 (dbGaP accession: phs001657**)**, ESAML (dbGaP accession: phs001027)**,** and GAML (dbGaP: phs000159). miRNA data were obtained from TCGA-LAML and GAML cohorts.

For TCGA-LAML, BEATAML2.0, and ESAML cohorts, we generated updated ELN-2022 risk classifications using a reproducible rule-based framework implemented in R-v4.3 and consistent with the criteria described by Döhner et al. (2022) (3). Clinical, cytogenetic, and mutational annotations were harmonized to derive uniform prognostic categories across datasets. Each patient was then assigned to Favorable, Intermediate, or Adverse risk groups following the new ELN-2022 criteria. The complete computational workflow and rule definitions are provided in the Supplementary Method.

Gene expression data were obtained as raw read counts and renormalized within each cohort using the Upper Quartile (UQ) method (48), followed by $\log_2$-transformation. Raw miRNA sequencing reads were trimmed (3′ adapter sequence: AGATCGGAAGAGCACACGTCT), filtered if shorter than 15 base pairs, collapsed, and quantified using miRDeep2 by aligning to known human mature and precursor miRNAs sequences (49). miRNA raw reads counts were normalized using the `calcNormFactors` function in edgeR-v4.4.2 with the Trimmed Mean of M-values (TMM) method (50), followed by $\log_2$-transformation. To reduce background noise and focus on reliably expressed transcripts, genes and miRNAs with average expression levels < 1 CPM (51) were excluded.

Demographic covariates

To account for potential demographic confounding, we examined the distribution and prognostic relevance of age, sex, and ethnicity across ELN-defined risk groups. Age differences were assessed using the Kruskal–Wallis rank-sum test, while categorical variables (sex and ethnicity) were evaluated using chi-square tests of independence. Age was further dichotomized into Young ($\leq$ 60 years) and Elder (> 60 years) groups. Kaplan–Meier survival analyses were performed with log-rank tests.

To address missing or incomplete ethnicity data in the BEATAML2.0 cohort, we created a Merged Ethnicity variable by hierarchically combining available sources. Specifically, inferred ethnicity variable was prioritized when available; if missing, self-reported race was used as a substitute. If both were unavailable, reported ethnicity was used as a fallback. This strategy ensured maximal data retention while preserving consistency in downstream covariate-adjusted analyses.

Two-step PCA–based survival feature selection

PCA was performed on each normalized expression matrix using the `prcomp` function in R to capture dominant and subtle sources of variation and reduce noise and dimensionality. The top 20 principal components (PCs), explaining > 50% of cumulative variance, were retained. Covariate-adjusted survival modeling was then conducted using Cox proportional hazards

regression, incorporating PCs as predictors and adjusting for age, sex, and ethnicity. PCs significantly associated with overall survival (BH-adjusted $p < 0.05$) were selected for downstream analyses. For each significant PC, the top 300 genes with the highest absolute loadings were extracted following the approach of Pollen et al., (2014) (52). A second PCA-based survival analysis was performed within each ELN risk group to mitigate risk-related confounding, and the top 100 survival-associated genes were extracted per ELN category. This two-stage PCA–survival framework enabled risk-aware prioritization of prognostic candidates. Genes showing consistent hazard-ratio patterns across both TCGA-LAML and BEATAML2.0 were then retained as reproducible prognostic biomarkers.

For miRNA analysis, the same analytical workflow was applied to TCGA-LAML. In the GAML cohort, which lacked ELN risk annotation, but included Tumor and Normal samples, differential expression analysis was performed using the Wilcoxon rank-sum test. Significant miRNAs (BH-adjusted $p < 0.05$) were then compared to those identified in TCGA-LAML to determine reproducible regulatory features.

Supervised classification and model validation

To evaluate the predictive power of the selected gene and miRNA features, supervised classification was conducted using SVM models, selected for their robustness against overfitting and capacity to handle high-dimensional feature spaces.

SVM models were trained on TCGA-LAML using established biomarkers, novel candidates, and combined feature sets, and top predictors were selected based on SVM importance scores. These optimized features were then validated across independent cohorts to assess reproducibility: gene-based models were tested in BEATAML2.0, ESAML, and GAML, while miRNA-based models were evaluated in GAML. Since GAML only contains Tumor versus Normal categories, classification was performed on Tumor versus Normal samples.

Model performance was assessed using five-fold cross-validation. For each fold, predicted labels were compared against true class assignments and categorized as true positives (TP), true negatives (TN), false positives (FP), and false negatives (FN). Classification performance was summarized using accuracy, precision, recall, F1 score, specificity, and AUC, defined as follows:

- **Accuracy** measures the proportion of correctly classified samples among all predictions:

$$\text{Accuracy} = \frac{\text{TP} + \text{TN}}{\text{TP} + \text{TN} + \text{FP} + \text{FN}}$$

- **Precision** represents the proportion of true positives among all positive predictions:

$$\text{Precission} = \frac{\text{TP}}{\text{TP} + \text{FP}}$$

- **Recall (Sensitivity)** reflects the proportion of actual positives correctly identified:

$$\text{Recall} = \frac{\text{TP}}{\text{TP} + \text{FN}}$$

- **Specificity** represents the proportion of true negatives correctly identified among all negative cases:

$$\text{Specificity} = \frac{\text{TN}}{\text{TN} + \text{FP}}$$

- **F1 Score** is the harmonic mean of precision and recall, offering a balanced metric when class distribution is imbalanced:

$$\text{F1 score} = 2 \times \frac{\text{Precision} \times \text{Recall}}{\text{Precision} + \text{Recall}}$$

- **AUC** is a threshold-independent measure of model performance, representing the probability that the classifier ranks a randomly chosen positive instance higher than a randomly chosen negative one.

To benchmark the effectiveness of our feature selection strategy, performance was compared against baseline models trained on randomly selected gene sets of the same size.

miRNA:gene regulatory interaction analysis

To investigate post-transcriptional regulatory mechanisms contributing to AML progression, we integrated experimentally validated miRNA:gene interactions with matched expression data. Validated miRNA:target pairs were obtained from TarBase-v9.0 (27), a curated database containing interactions supported by strong experimental evidence.

Using these curated pairs, we performed Spearman correlation analysis between miRNA and gene expression levels within matched patient samples. This non-parametric approach was chosen for its robustness to outliers and ability to capture monotonic relationships. Interactions with absolute Spearman correlation coefficients ($|\rho|$) ≥ 0.1 and p value < 0.05 were considered statistically significant and retained for downstream analyses. These correlation-filtered miRNA:gene pairs were then integrated into the SVM classification framework, with models trained in TCGA-LAML and validated in the independent GAML cohort to assess cross-cohort reproducibility and predictive performance.

Cox regression–based patient risk score calculation

To quantify the prognostic relevance of integrated miRNA:gene biomarkers, we fitted a Cox proportional hazards model using expression values from the selected miRNA:gene pairs. For each patient i, a continuous risk score was computed as:

$$\text{Risk Score}_i = \sum_j \beta_j \times \text{Expression}_{ij},$$

where β_j represents the Cox regression coefficient for biomarker j. Model performance was assessed with five-fold cross-validation, then a final model was fit to the full TCGA-LAML cohort to derive stable β_j estimates and patient-level risk scores. Patients were classified into High and Low risk using the median score for downstream survival evaluation with ELN-2022.

Assessment of added prognostic value beyond ELN-2022

To evaluate whether the proposed molecular risk score provides additional prognostic information beyond the ELN-2022 classification, we fitted a series of Cox proportional hazards models to overall survival in the TCGA-LAML cohort. All models were expressed as:

$$h(t) = h_0(t)\exp(\eta),$$

where $h_0(t)$ is the baseline hazard function and η represents the linear predictor composed of clinical and molecular covariates. Model performance was evaluated using AIC, with improvements determined by comparing AIC values across models. The model with the lowest AIC was considered to provide the best balance between explanatory power and model complexity.

A baseline Cox model was first constructed using established clinical predictors, including age category, sex, and ELN-2022 risk classification, including Favorable, Intermediate and Adverse groups:

$$\text{Model 1: } h(t) = h_0(t)\exp(\beta_1 \cdot \text{AGE CATEGORY} + \beta_2 \cdot \text{SEX} + \beta_3 \cdot \text{ELN RISK})$$

This model served as the reference for evaluating added prognostic value. To test whether the continuous molecular risk score contributed independent information, we extended the baseline model by adding the score as a covariate:

$$\text{Model 2: } h(t) = h_0(t)\exp(\beta_1 \cdot \text{AGE CATEGORY} + \beta_2 \cdot \text{SEX} + \beta_3 \cdot \text{ELN RISK} + \beta_4 \cdot \text{RISK SCORE})$$

Model improvement was evaluated by comparing AIC values between the ELN-only and extended models.

To directly compare categorical prognostic groupings, we dichotomized the molecular risk score at its optimized threshold to define High- and Low-risk groups. Two Cox models were then fitted, one using ELN Favorable/Adverse categories and the other using molecular High/Low groups:

$$\text{Model 3A: } h(t) = h_0(t)\exp(\beta_1 \cdot \text{AGE CATEGORY} + \beta_2 \cdot \text{SEX} + \beta_3 \cdot \text{ELN RISK})$$
$$\text{Model 3B: } h(t) = h_0(t)\exp(\beta_1 \cdot \text{AGE CATEGORY} + \beta_2 \cdot \text{SEX} + \beta_3 \cdot \text{RISK GROUP})$$

Comparison of AIC values between Models 3A and 3B allowed us to assess whether molecular risk groups better explained survival outcomes than ELN categories.

To dissect the contribution of the molecular components underlying the risk score, additional Cox models were constructed using the set of miRNAs and genes from the 10 miRNA:gene pairs, alongside the clinical predictors:

$$\text{Model 4A: } h(t) = h_0(t)\exp\left(\beta_1 \cdot \text{AGE CATEGORY} + \beta_2 \cdot \text{SEX} + \beta_3 \cdot \text{ELN RISK} + \sum_j \beta_j \cdot \text{MARKER}_j\right)$$

$$\text{Model 4B: } h(t) = h_0(t)\exp\left(\beta_1 \cdot \text{AGE CATEGORY} + \beta_2 \cdot \text{SEX} + \sum_j \beta_j \cdot \text{MARKER}_j\right)$$

Finally, to assess whether a gene-only panel could capture survival variation independent of ELN, we constructed gene-only models with and without ELN:

$$\text{Model 5A: } h(t) = h_0(t)\exp\left(\beta_1 \cdot \text{AGE CATEGORY} + \beta_2 \cdot \text{SEX} + \beta_3 \cdot \text{ELN RISK} + \sum_j \beta_j \cdot \text{GENE}_j\right)$$

$$\text{Model 5B: } h(t) = h_0(t)\exp\left(\beta_1 \cdot \text{AGE CATEGORY} + \beta_2 \cdot \text{SEX} + \sum_j \beta_j \cdot \text{GENE}_j\right)$$

These models allowed us to determine whether gene-level information alone explained survival differences beyond the ELN classification.

Then, all analyses were replicated in the independent BEATAML2.0 cohort using the same modeling framework to validate the generalizability and prognostic robustness of the molecular risk score.

Data Availability

TCGA-LAML RNA- and miRNA- sequencing data, along with clinical annotations, are publicly available via the NCI Genomic Data Commons (Project ID: TCGA-LAML, Program: TCGA). BEATAML2.0 RNA- sequencing data are accessible through dbGaP (accession ID: phs001657). ESAML RNA- sequencing data are accessible through dbGaP (accession ID: phs001027). GAML RNA/small RNA-sequencing data are available via dbGaP (accession ID: phs000159).

Authors' Contributions

T.G. conceived and supervised the study. D.B. acquired and preprocessed the data. D.H.G. performed the analyses. T.G. and D.H.G. interpreted the results and wrote the manuscript. All authors reviewed, edited, and approved the final version.

Conflict-of-interest disclosure: The authors declare no competing financial interests.

ORCHID profiles: D.H.G., 0009-0005-1906-4308. D.B., 0000-0002-1744-1668. T.G., 0000-0002-8379-0962.

Acknowledgments

We thank Drs. Timothy J. Ley and Christopher A. Miller (Washington University); Richard Corbett, and Drs. Emilia Lim and Marco Marra (University of British Columbia) for their invaluable assistance in acquiring the gene and miRNA datasets. This work was supported, in part, by Institutional Research Grant IRG #22-151-37-IRG from the American Cancer Society and by the Medical College of Wisconsin (MCW) Cancer Center.

Notes

The code used for data processing and analysis is available at https://github.com/tjgu/AML-miRNA-RNA-biomarker-discovery.git

References

1. Papaemmanuil E, Gerstung M, Bullinger L, Gaidzik VI, Paschka P, Roberts ND, et al. Genomic classification and prognosis in acute myeloid leukemia. New England Journal of Medicine. 2016 Jun 9;374(23):2209-21.
2. Döhner H, Estey E, Grimwade D, Amadori S, Appelbaum FR, Büchner T, et al. Diagnosis and management of AML in adults: 2017 ELN recommendations. Blood. 2017;129(4):424-447.
3. Döhner H, Wei AH, Appelbaum FR, Berman E, Brune JL, Crysandt M, et al. Diagnosis and management of AML in adults: 2022 ELN recommendations. Blood. 2022;140(12):1345-1377.
4. Shafiei FS, Abroun S, Vahdat S, Bidad K, Nosrati A, Montazer F, et al. Identification of prognostic-related genes in AML: a study based on TCGA data analysis. Biochem Genet. 2025;63:11193.
5. Marcucci G, Radmacher MD, Maharry K, Mrozek K, Ruppert AS, Paschka P, et al. MicroRNA expression in cytogenetically normal AML. N Engl J Med. 2008;358:1919-1928.
6. Marcucci G, Mrózek K, Radmacher MD, Garzon R, Bloomfield CD. The prognostic and functional role of microRNAs in AML. Blood. 2011;117(4):1121-1129.
7. Moison C, Spinella JF, Chagraoui J, Mayotte N, Bystrykh LV, Willams LA, et al. HMGA2 expression defines a subset of human AML with immature transcriptional signature and vulnerability to G2/M inhibition. Blood Adv. 2022;6(16):4793–4806.
8. Tan L, Wei X, Zheng L, Zhao W, Zhang S, Wang J. Amplified HMGA2 promotes cell growth by regulating Akt pathway in AML. J Cancer Res Clin Oncol. 2016;142:389–399.
9. Pasalic Z, Greif PA, Jurinovic V, Garcia-Manero G, Schnittger S, Haferlach C, et al. FHL2 interacts with CALM and is highly expressed in acute erythroid leukemia. Blood Cancer J. 2011;1:e42.
10. Lu W, Yu T, Liu S, Luo R, Guo L, Xu L, et al. FHL2 interacts with Iaspp and impacts the biological functions of leukemia cells. Blood. 2016;128(22):5111.
11. Li H, Li J, Cheng J, Zhang X, Xie C, Zhao Z, et al. AML-derived mesenchymal stem cells upregulate CTGF expression through the BMP pathway. Oncol Rep. 2019;42(3):1035–1046.
12. Ayala RM, Martínez-López J, Albízua E, Gómez-Casares MT, López-Jiménez J, Sarasquete ME, et al. Clinical significance of GATA1 expression in AML. Am J Hematol. 2009;84(2):79–86.
13. Caldwell JT, Edwards H, Dombkowski AA, Doan PL, McGraw KL, Hardaway JA, et al. Overexpression of GATA1 confers resistance to chemotherapy in AMKL. PLoS One. 2013;8(7):e68601.
14. Qiang P, Pan Q, Fang C, Fozza C, Song K, Dai Y, et al. MicroRNA-181a-3p as a diagnostic and prognostic biomarker for acute myeloid leukemia. Mediterr J Hematol Infect Dis. 2020;12(1):e2020012.
15. Wallace JA, O'Connell RM. MicroRNAs and acute myeloid leukemia: therapeutic implications and emerging concepts. Blood. 2017;130(11):1290–1301.

16. Guo Q, Liu J, Han X, Chen S, Guo L, Liu N, et al. MicroRNA-181 as a prognostic biomarker for survival in acute myeloid leukemia: a meta-analysis. Oncotarget. 2017;8(44):76102–76113.
17. Trino S, Lamorte D, Caivano A, de Luca L, Sgueglia G, Laurenzana I, et al. MicroRNAs as new biomarkers for diagnosis and prognosis, and as potential therapeutic targets in acute myeloid leukemia. Int J Mol Sci. 2018;19(2):460.
18. Liao Q, Wang B, Li X, Jiang G. miRNAs in acute myeloid leukemia. Oncotarget. 2016;8(2):3666.
19. Fletcher D, Brown E, Javadala J, Uysal-Onganer P, Guinn BA. microRNA expression in acute myeloid leukaemia: New targets for therapy? EJHaem. 2022;3(3):596-608.
20. Li J, Wang S. Integrative analysis of epigenetic subtypes in AML: A multi-center study combining machine learning for prognostic and therapeutic insights. PLoS One. 2025;20(5):e0324380.
21. Erkers T, Marabita F, Struyf N, Dander E, Undurraga AM, Rorby E, et al. Data-driven molecular hallmarks of AML: biological, prognostic and therapeutic implications. Blood. 2022;140(Suppl 1):6299.
22. Cortes C, Vapnik V. Support-vector networks. Mach Learn. 1995;20(3):273-297.
23. Vagapova ER, Spirin PV, Lebedev TD, Prassolov VS. The role of TAL1 in hematopoiesis and leukemogenesis. Acta Naturae (англоязычная версия). 2018;10(1 (36)):15-23.
24. Taghiloo S et al. Immune evasion mechanisms in acute myeloid leukemia. Crit Rev Oncol Hematol, 2021.
25. Chen Y, Li J, Xu L, Găman MA, Zou Z. The genesis and evolution of acute myeloid leukemia stem cells in the microenvironment: From biology to therapeutic targeting. Cell Death Discovery. 2022 Sep 26;8(1):397.
26. Mansoori B, Mohammadi A, Ditzel HJ, Duijf PH, Khaze V, Gjerstorff MF, Baradaran B. HMGA2 as a critical regulator in cancer development. Genes. 2021 Feb 13;12(2):269.
27. Skoufos G, Kakoulidis P, Tastsoglou S, Kanakaris N, Alexiou P, Vlachos IS, et al. TarBase v9.0 extends experimentally supported miRNA–gene interactions. Nucleic Acids Res. 2024;52(D1):D304-D310.
28. Guo J, Zhang R, Yang Z, Jiang Y, Sun D, Ma J, et al. Biological roles and therapeutic applications of IDH2 mutations in human cancer. Front Oncol. 2021;11:644857.
29. Burnham KP, Anderson DR, editors. Model selection and multimodel inference: a practical information-theoretic approach. New York, NY: Springer New York; 2002 Jul.
30. Ng SW, Mitchell A, Kennedy JA, Chen WC, McLeod J, Ibrahimova N, et al. A 17-gene stemness score for rapid determination of risk in acute leukaemia. Nature. 2016;540:433–437.
31. Lai B, Lai Y, Zhang Y, Zhou M, OuYang G. Survival prediction in acute myeloid leukemia using gene expression profiling. BMC Medical Informatics and Decision Making. 2022 Mar 3;22(1):57.
32. Ellson I, Martorell-Marugán J, Carmona-Sáez P, Ramos-Mejia V. MiRNA expression as outcome predictor in pediatric AML: systematic evaluation of a new model. NPJ Genomic Medicine. 2024 Aug 6;9(1):40.
33. Yacob AM, Al-Mahmood S, Hassan R, Qamar R, Alshahrani M, Alshamrani S, et al. Hsa-miR-181a-5p, hsa-miR-182-5p, and hsa-miR-26a-5p as biomarkers in leukemia. BMC Cancer. 2022;22:332.
34. Otmani K, Lewalle P. Tumor suppressor miRNA in cancer cells and the tumor microenvironment. Front Oncol. 2021;11:708765.
35. Galli T, Le Borgne R, Langley K, Marteil G, Vacher J, Louvard D, et al. Malectin is a conserved glycoprotein quality control receptor in the endoplasmic reticulum. Proc Natl Acad Sci USA. 2011;108(18):7517–7522.

36. Lu Y, et al. Role of endoplasmic reticulum stress response in leukemia progression. Leuk Res. 2012;36(7):894–900.
37. Gong Z, Wang W, He Y, Zhou J, Yang Q, Feng A, et al. Integrated Multi-Omics Analysis Identifies SRI as a Critical Target Promoting Gastric Cancer Progression and Associated with Poor Prognosis. Cancers. 2025 Oct 29;17(21):3483.
38. Li Z, Huang H, Li Y, Liu D, Wang Y, Chen P, et al. Up-regulation of a HOXA-PBX3 homeobox-gene signature following down-regulation of miR-181 is associated with adverse prognosis in patients with cytogenetically abnormal AML. Blood. 2012;119(10):2314–2324.
39. Su R, Lin HS, Zhang XH, Zhao J, Wang J, Chen J, et al. MiR-181 family: regulators of myeloid differentiation and acute myeloid leukemia as well as potential therapeutic targets. Oncogene. 2015;34(25):3226–3239.
40. Yang Y, Li F, Saha MN, Abdi J, Qiu L, Chang H. miR-3613-5p promotes tumor progression in non-small cell lung cancer by targeting SOCS2. Oncotarget. 2018;9(5):5073–5086.
41. Bi J, Wang Y, Wang Y. MiR-3613-5p targets AQP4 to promote the progression of chronic atrophic gastritis to gastric cancer. Frontiers in Pharmacology. 2025 Apr 4;16:1523689.
42. Liu J, Wang Y, Meng H, Wang R, Li Q, Yu X, et al. MicroRNA-3613-5p promotes breast cancer cell proliferation and invasion by targeting the tumor suppressor gene PTEN. Biochem Biophys Res Commun. 2019;508(3):728–734.
43. Szklarczyk D, Gable AL, Nastou KC, Lyon D, Kirsch R, Pyysalo S, et al. The STRING database in 2021: customizable protein–protein networks, and functional characterization of user-uploaded gene/measurement sets. Nucleic Acids Res. 2021;49(D1):D605–D612.
44. Johansson J, Gidlöf O, Gidlöf S, Olsson A, Richter J, Wennberg M, et al. The LIM-only protein FHL2 is a co-activator of β-catenin and promotes proliferation in hematopoietic cells. Blood. 2009;114(12):2443–2451.
45. Feng Y, Wei F, Zhang X, Wang Y, Cheng Y, Li X, et al. FHL2 promotes tumor progression and is a predictor of poor prognosis in acute myeloid leukemia. OncoTargets Ther. 2019;12:4565–4576.
46. Corder EH, Saunders AM, Strittmatter WJ, Schmechel DE, Gaskell PC, Small GW, et al. Gene dose of apolipoprotein E type 4 allele and the risk of Alzheimer's disease in late onset families. Science. 1993;261(5123):921–923.
47. Mahley RW, Rall SC Jr. Apolipoprotein E: far more than a lipid transport protein. Annu Rev Genomics Hum Genet. 2000;1:507-537.
48. Bullard JH, Purdom E, Hansen KD, Dudoit S. Evaluation of statistical methods for normalization and differential expression in mRNA-Seq experiments. BMC Bioinformatics. 2010;11:94.
49. Friedländer MR, Mackowiak SD, Li N, Chen W, Rajewsky N. miRDeep2 accurately identifies known and hundreds of novel microRNA genes in seven animal clades. Nucleic Acids Res. 2012;40(1):37–52.
50. Robinson MD, Oshlack A. A scaling normalization method for differential expression analysis of RNA-seq data. Genome Biol. 2010;11(3):R25.
51. Chen Y, Lun ATL, Smyth GK. From reads to genes to pathways: differential expression analysis of RNA-seq experiments using Rsubread and edgeR. F1000Res. 2016;5:1438.
52. Pollen AA, Nowakowski TJ, Shuga J, Wang X, Leyrat A, Lui JH, et al. Low-coverage single-cell mRNA sequencing reveals cellular heterogeneity and activated signaling pathways in developing cerebral cortex. Nat Biotechnol. 2014;32(10):1053–1058.
53. Lengliné E. C1q helps AML to disseminate and resist. Blood. 2023;141(7):691–692.
54. Korbecki J, Kupnicka P, Barczak K, Majewski P, Polak J, Chmielowiec J, et al. The role of CXCR1, CXCR2, CXCR3, CXCR5, and CXCR6 ligands in AML. Cancers. 2023;15(18):4555.

55. Abd El-Hassib DM, El-Shennawy D, El-Nashar NE, Omar MA, Hussein G, Farag Y. Study of MicroRNA-181a-3p as a biomarker for diagnosis of AML. Egypt J Hosp Med. 2023;91:4780–4785.
56. Luo LJ, Wang DD, Wang J, Yang F, Tang JH. Diverse roles of miR-335 in development and progression of cancers. Tumor Biol. 2016;37(12):15399–410.
57. Otmani K, Lewalle P. Tumor suppressor miRNA in cancer cells and the tumor microenvironment. Front Oncol. 2021;11:708765.
58. Chen H, Wang J, Wang H, Liang J, Dong J, Bai H, et al. Advances in the application of Let-7 microRNAs in the diagnosis, treatment and prognosis of leukemia. Oncol Lett. 2022;23(1):1.
59. Chirshev E, Oberg KC, Ioffe YJ, Unternaehrer JJ. Let-7 as biomarker, prognostic indicator, and therapy for precision medicine in cancer. Clin Transl Med. 2019;8(1):24.
60. Xiang Y, Tian Q, Guan L, Niu SS. The dual role of miR-186 in cancers: Oncomir battling with tumor suppressor miRNA. Front Oncol. 2020;10:233.
61. Liu Y, Liu J, Feng Y, Xu X, Miao Y, Chen H, et al. Prognostic value of miR-106a and miR-20a in AML patients with chemotherapy or allo-HSCT treatment. Hematology. 2025;30(1):2533577.
62. Sperb N, Krowiorz K, Grasedieck S, Rueß C, Pochert N, Schneider E, et al. Members of the microRNA-106a-363 cluster associate with unfavorable outcome in adult acute myeloid leukemia and promote leukemogenesis in vivo through increased metabolic activity. Blood. 2018;132:3924.
63. Mirzaei Z, Barati T, Ebrahimi A, Derakhshan SM, Khaniani MS. The role of miR-7-5p in cancer: function, prognosis, diagnosis, and therapeutic implications. Mol Biol Rep. 2025;52(1):12.
64. Muys BR, Sousa JF, Placa JR, de Araujo LF, Sarshad AA, Anastasakis DG, et al. miR-450a acts as a tumor suppressor in ovarian cancer by regulating energy metabolism. Cancer Res. 2019;79(13):3294–305.
65. Chen L, Jiang X, Chen H, Han Q, Liu C, Sun M. RETRACTED ARTICLE: microRNA-628 inhibits proliferation of acute myeloid leukemia cells by directly targeting IGF-1R. OncoTargets Ther. 2019:907–19.
66. Jiang N, Jiang X, Chen Z, Song X, Wu L, Zong D, et al. miR-203a-3p suppresses cell proliferation and metastasis by inhibiting LASP1 in nasopharyngeal carcinoma. J Exp Clin Cancer Res. 2017;36(1):138.
67. Gillen AE, Yamamoto TM, Kline E, Hesselberth JR, Kabos P. Improvements to the HITS-CLIP protocol eliminate widespread mispriming artifacts. BMC genomics. 2016 May 5;17(1):338.
68. Muys BR, Sousa JF, Plaça JR, de Araujo LF, Sarshad AA, Anastasakis DG, et al. miR-3613-5p regulates ovarian cancer cell proliferation. Oncotarget. 2019;10(15):1514–1524.
69. Yu F, Yao H, Zhu P, Zhang X, Pan Q, Gong C, et al. let-7 regulates self-renewal and tumorigenicity of breast cancer cells. Cancer Res. 2015;75(3):706–715.
70. Fields CJ, Herndon JM, Gustafson DL, Armistead PM, Larsen H, Samuel M, et al. qCLASH reveals widespread miRNA–mRNA interactions in colorectal cancer. RNA Biol. 2021;18(10):1570–1582.
71. Gay LA, Sethuraman S, Thomas M, Donnell OC, Withey S, Trabold K, et al. Kaposi's sarcoma-associated herpesvirus infection alters endothelial cell microRNA expression. J Virol. 2018;92(2):e01874-17.
72. Gottwein E, Mukherjee N, Sachse C, Frenzel C, Majoros WH, Chi J, et al. A viral microRNA functions as an orthologue of cellular miR-155. Cell Host Microbe. 2011;9(2):139–150.
73. Pillai MM, Gillen AE, Yamamoto TM, Kline D, Brown MR, Tomar T, et al. Hsa-miR-942-5p regulates tumorigenicity in breast cancer cells. Breast Cancer Res. 2014;16(6):467.

74. Boudreau RL, Jiang P, Gilmore BL, Spengler RM, Tirabassi R, Nelson JA, et al. Transcriptome-wide discovery of microRNA binding sites in human brain. Nat Neurosci. 2014;17(12):1631–1639.
75. Hamilton MP, Rajapakshe K, Bader DA, Meeker AK, Wadsworth JT, Zhao S, et al. The miR-3613-5p regulates prostate cancer cell growth by targeting key cell cycle regulators. Cancer Lett. 2016;373(2):303–311.
76. Kameswaran V, Bramswig NC, McKenna LB, Penn M, Schug J, Hand NJ, et al. Epigenetic regulation of the DLK1-MEG3 microRNA cluster in human type 2 diabetes. Diabetes. 2014;63(2):639–647.
77. Karginov FV, Hannon GJ. Remodeling of microRNA target mRNAs in human kidney cells. Genome Res. 2013;23(1):1–14.
78. Skalsky RL, Samols MA, Plaisance KB, Boss IW, Riva A, Lopez MC, et al. Kaposi's sarcoma–associated herpesvirus encodes an ortholog of miR-155. PLoS Pathog. 2012;8(4):e1002512.
79. Snaith O, Poveda-Rogers C, Laczko D, Yang G, Morrissette JJD. Cytogenetics and genomics of acute myeloid leukemia. Best Pract Res Clin Haematol. 2024;37(1):101533. doi:10.1016/j.beha.2023.101533.
80. Wolman SR, Gundacker H, Appelbaum FR, Slovak ML; Southwest Oncology Group. Impact of trisomy 8 (+8) on clinical presentation, treatment response, and survival in acute myeloid leukemia: a Southwest Oncology Group study. Cancer Genet Cytogenet. 2002;133(2):118–125. doi:10.1016/S0165-4608(01)00648-2.

Figure captions

Figure 1: Clinical characteristics and survival associations in the TCGA-LAML cohort. (A) Overall survival differed significantly across ELN-defined Favorable, Intermediate, and Adverse risk categories, with Kaplan–Meier analysis confirming distinct survival patterns by ELN group (B, p value< 0.0001). (C) Age distribution varied across ELN categories, and survival analysis by age group (<60 vs ≥60 years) demonstrated markedly poorer outcomes in older patients (D, p value < 0.0001).

Figure 2: Workflow for prognostic biomarker discovery. This schematic summarizes the analytical pipeline used to identify prognostic biomarkers across multiple molecular layers. Gene-specific, miRNA-specific, and miRNA:gene paired features were independently evaluated using SVM classifiers and survival analyses. Significant features from each layer were then integrated to construct a Cox regression–derived risk score, yielding a unified molecular predictor of AML patient outcomes.

Figure 3: Cross-cohort predictive performance of prognostic genes in AML. (A) ROC curves from SVM models trained on the TCGA-LAML cohort and validated across three independent cohorts, BEATAML2.0, ESAML and GAML, demonstrating the robustness of known, novel, combined, and top-ranked prognostic gene sets. (B) Evaluation metrics—including accuracy, precision, recall, F1 score, and specificity—for the TCGA-LAML-trained models applied to external validation datasets. (C) ROC curves from models trained on the BEATAML2.0 cohort and validated on TCGA-LAML, assessing bidirectional predictive generalizability. (D) Corresponding evaluation metrics for BEATAML2.0–trained models tested on TCGA-LAML. (E) Violin plots showing expression differences of selected top-ranked genes across ELN risk groups, with red bars indicating group means. Others are shown in Supplementary Fig. S8. Asterisks (*) denote miRNAs previously reported in AML.

Figure 4: Predictive performance of prognostic miRNAs in AML. (A) ROC curves generated from SVM models trained on TCGA-LAML using known, novel, combined, and top-ranked

miRNAs, and validated in an independent cohort, GAML. (B) Evaluation metrics—including accuracy, precision, recall, F1 score, and specificity—for each miRNA-based model. (C) Violin plot showing expression differences of selected top-ranked miRNAs across ELN risk groups, with red bars indicating group means. Others are shown in Supplementary Fig. S12. Asterisks (*) denote miRNAs previously reported in AML.

Figure 5: Integrated miRNA:target regulatory patterns and cross-cohort predictive performance in AML. (A) Scatterplot, violin plot, and schematic pathway panel illustrating the inverse regulatory relationship between miR-181a-3p and MLEC. MLEC expression decreases while miR-181a-3p increases from favorable to adverse ELN risk groups. The mechanistic diagram depicts reduced miR-181a-3p leading to MLEC upregulation. (B) Scatterplot, violin plot, and schematic pathway panel illustrating the positive regulatory association between miR-3613-5p and FHL2, showing concordant increases across ELN categories. The mechanistic diagram highlights that elevated miR-3613-5p coincides with upregulation of FHL2. Scatterplots display $\log_2$-transformed CPM values with fitted regression lines, and violin plots depict expression distributions across ELN risk groups. (C) ROC curves for SVM models trained on TCGA-LAML and validated in the GAML cohort, comparing predictive performance using paired miRNAs alone, paired target genes alone, and combined miRNA:gene pairs. (D) Evaluation metrics—including accuracy, precision, recall, and F1 score—demonstrating that combined miRNA:target pairs achieve superior cross-cohort predictive accuracy relative to single-layer models.

Figure 6: Risk score–based survival prediction and clinical stratification in AML. (A) Kaplan–Meier plot showing overall survival differences between high- and low-risk groups defined by our molecular risk score. (B) Boxplots comparing survival distributions under traditional ELN-2022 categories (left) versus our risk-score–based stratification (right). Using a threshold of **0.021**, the TCGA-LAML cohort was dichotomized into Low and High risk within each ELN category, demonstrating improved within-category discrimination. (C) Survival stratification in the TCGA-LAML cohort comparing our risk score with the ELN-2022 system. Patients were dichotomized using a risk-score threshold, and the contingency table summarizes classification differences between the two systems. (D) Final Cox model β-coefficients used to compute the risk score, providing a practical formula for application to new patient data.

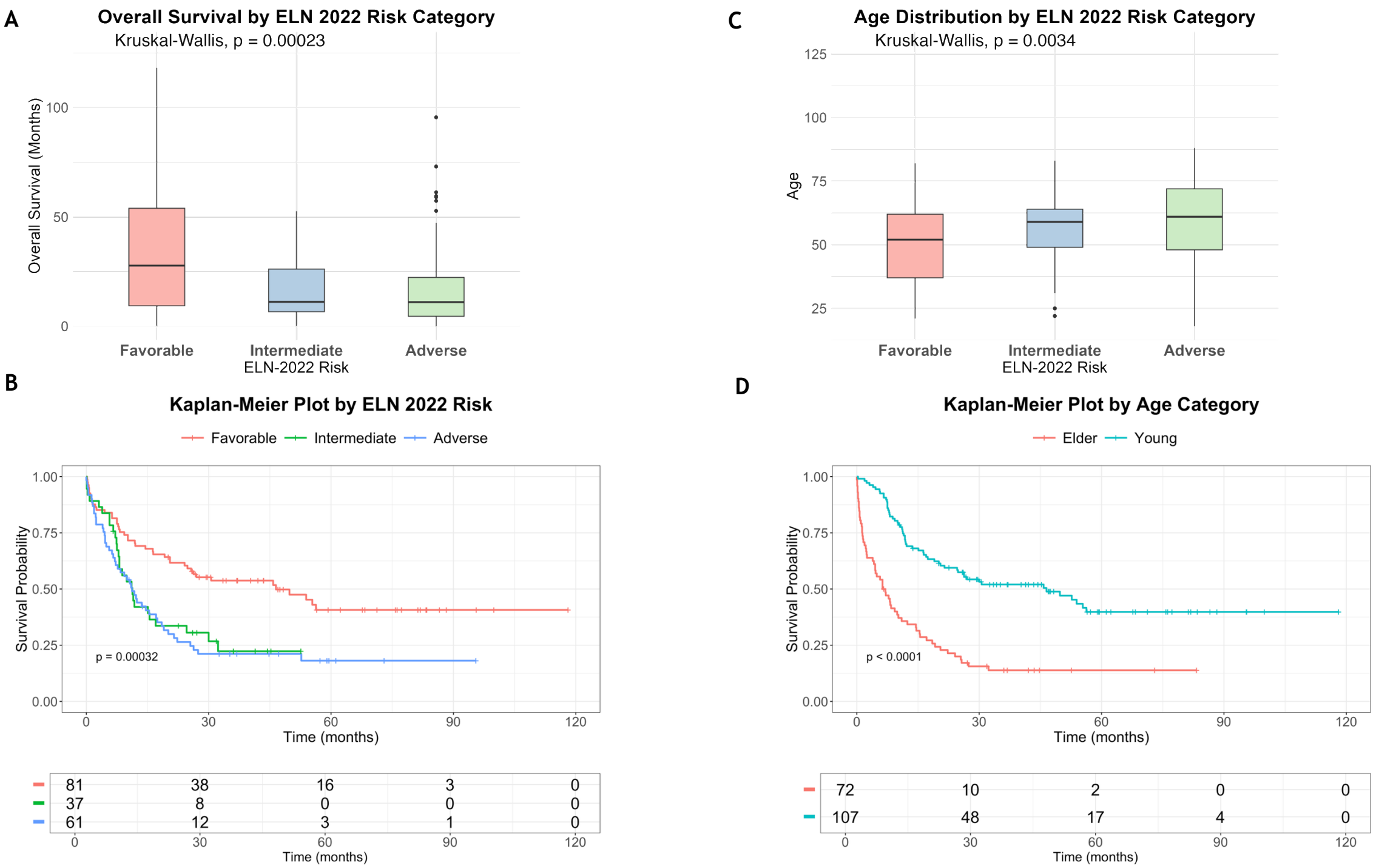
A
Overall Survival by ELN 2022 Risk Category
Kruskal-Wallis, p = 0.00023
Overall Survival (Months)
100
50
0
Favorable
Intermediate
Adverse
ELN-2022 Risk
C
Age Distribution by ELN 2022 Risk Category
Kruskal-Wallis, p = 0.0034
Age
125
100
75
50
25
Favorable
Intermediate
Adverse
ELN-2022 Risk
B
Kaplan-Meier Plot by ELN 2022 Risk
Favorable
Intermediate
Adverse
Survival Probability
1.00
0.75
0.50
0.25
0.00
p = 0.00032
0
30
60
90
120
Time (months)
81 38 16 3 0
37 8 0 0 0
61 12 3 1 0
Time (months)
D
Kaplan-Meier Plot by Age Category
Elder
Young
Survival Probability
1.00
0.75
0.50
0.25
0.00
p < 0.0001
0
30
60
90
120
Time (months)
72 10 2 0 0
107 48 17 4 0
Time (months)

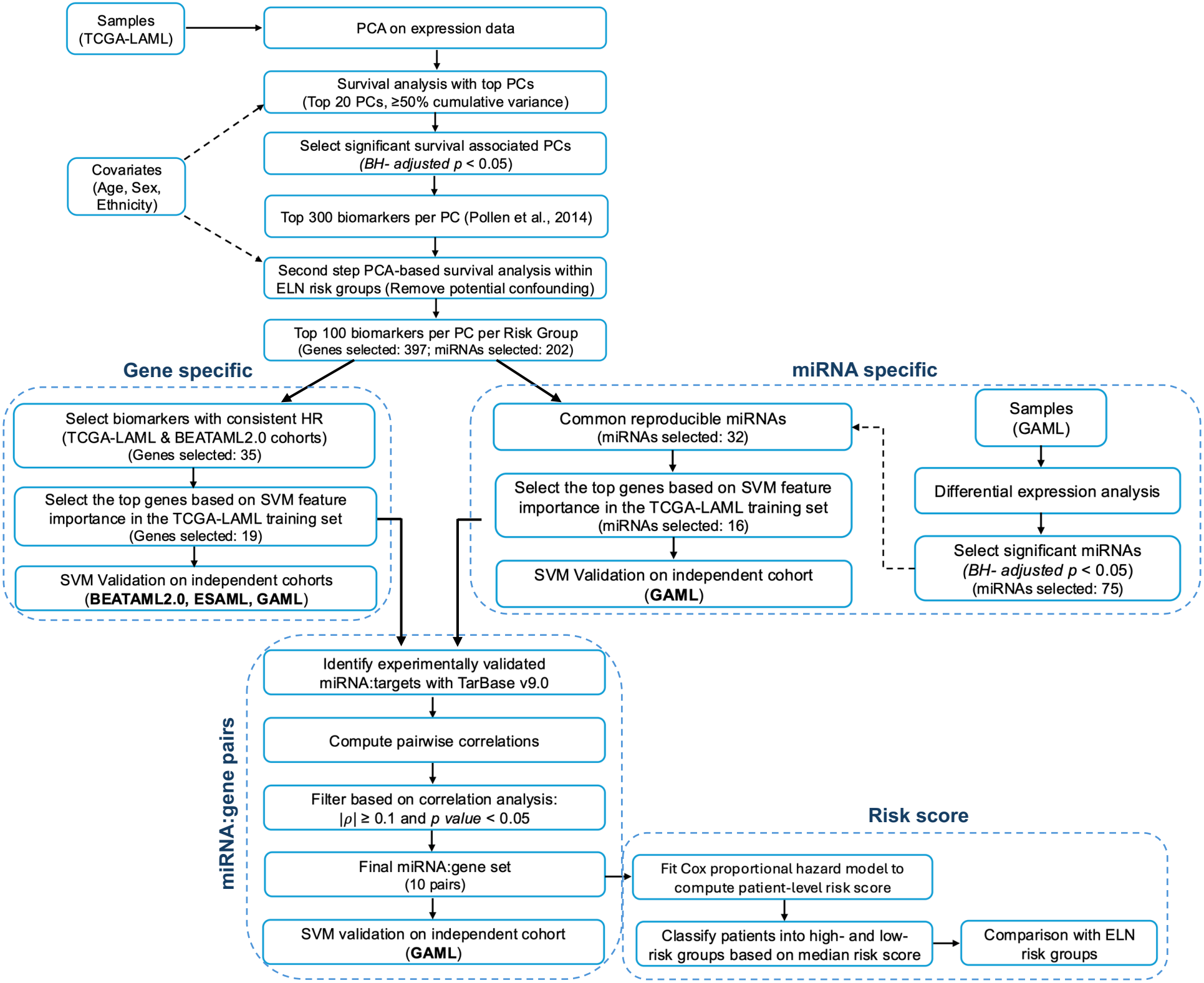
Samples (TCGA-LAML)
PCA on expression data
Survival analysis with top PCs (Top 20 PCs, ≥50% cumulative variance)
Select significant survival associated PCs (BH- adjusted p < 0.05)
Covariates (Age, Sex, Ethnicity)
Top 300 biomarkers per PC (Pollen et al., 2014)
Second step PCA-based survival analysis within ELN risk groups (Remove potential confounding)
Top 100 biomarkers per PC per Risk Group (Genes selected: 397; miRNAs selected: 202)
Gene specific
Select biomarkers with consistent HR (TCGA-LAML & BEATAML2.0 cohorts) (Genes selected: 35)
Select the top genes based on SVM feature importance in the TCGA-LAML training set (Genes selected: 19)
SVM Validation on independent cohorts (BEATAML2.0, ESAML, GAML)
miRNA specific
Common reproducible miRNAs (miRNAs selected: 32)
Select the top genes based on SVM feature importance in the TCGA-LAML training set (miRNAs selected: 16)
SVM Validation on independent cohort (GAML)
Samples (GAML)
Differential expression analysis
Select significant miRNAs (BH- adjusted p < 0.05) (miRNAs selected: 75)
miRNA:gene pairs
Identify experimentally validated miRNA:targets with TarBase v9.0
Compute pairwise correlations
Filter based on correlation analysis: |ρ| ≥ 0.1 and p value < 0.05
Final miRNA:gene set (10 pairs)
SVM validation on independent cohort (GAML)
Risk score
Fit Cox proportional hazard model to compute patient-level risk score
Classify patients into high- and low-risk groups based on median risk score
Comparison with ELN risk groups

A

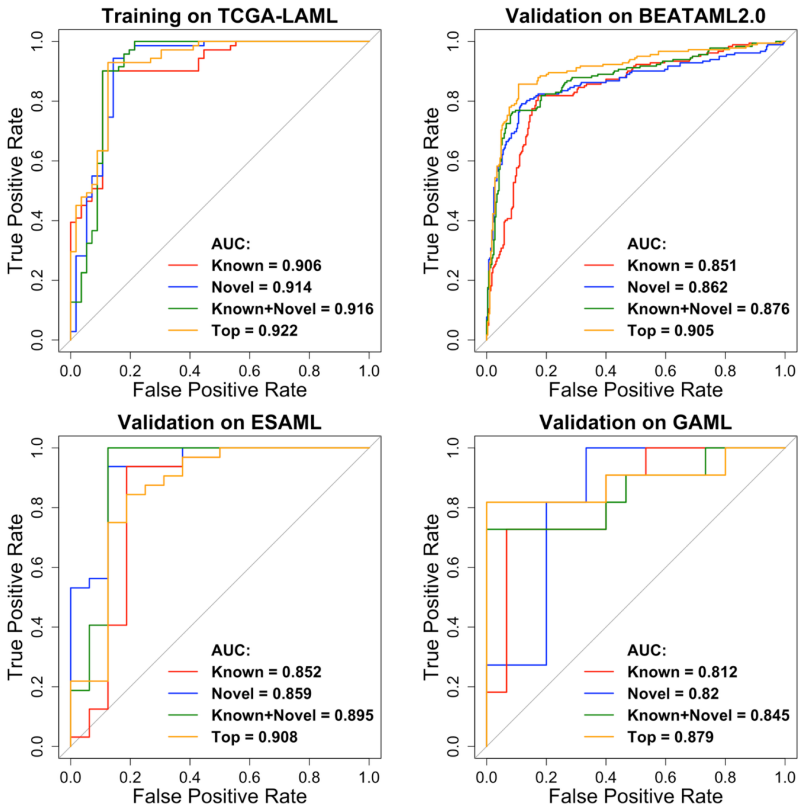

C

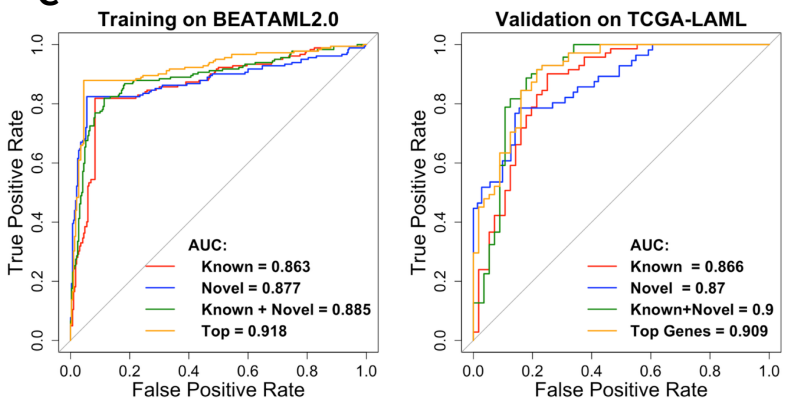

B

Genes	Accuracy	Precision	Recall	F1score	Specificity
Training on TCGA-LAML					
Known	0.9	0.88	0.89	0.88	0.9
Novel	0.9	0.91	0.86	0.88	0.94
All	0.9	0.88	0.89	0.88	0.9
Top	0.91	0.91	0.88	0.89	0.93
Validation on BEATAML2.0					
Known	0.82	0.85	0.85	0.85	0.76
Novel	0.84	0.84	0.89	0.87	0.74
All	0.85	0.85	0.87	0.86	0.78
Top	0.87	0.89	0.88	0.89	0.85
Validation on ESAML					
Known	0.8	0.8	0.75	0.77	0.9
Novel	0.85	0.77	0.81	0.79	0.88
All	0.88	0.78	0.88	0.82	0.88
Top	0.9	0.82	0.88	0.85	0.91
Validation on GAML					
Known	0.7	0.75	0.72	0.72	0.73
Novel	0.76	0.81	0.74	0.78	0.82
All	0.8	0.85	0.85	0.81	0.85
Top	0.82	0.85	0.85	0.85	0.87

D

Genes	Accuracy	Precision	Recall	F1score	Specificity
Training on BEATAML2.0					
Known	0.86	0.87	0.87	0.87	0.82
Novel	0.88	0.89	0.92	0.9	0.82
All	0.9	0.89	0.95	0.92	0.82
Top	0.92	0.93	0.95	0.94	0.88
Validation on TCGA-LAML					
Known	0.81	0.81	0.75	0.78	0.86
Novel	0.82	0.82	0.76	0.79	0.87
All	0.86	0.9	0.79	0.84	0.93
Top	0.88	0.87	0.84	0.85	0.9

E

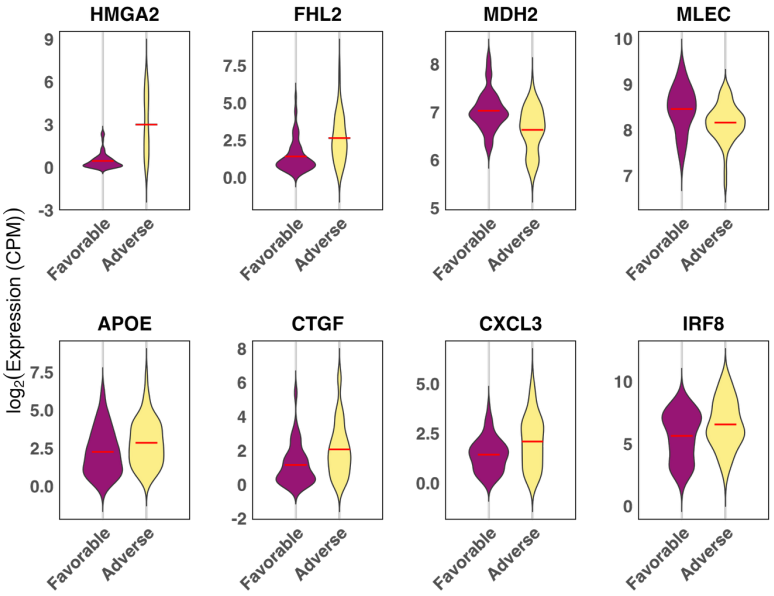

Top Genes: HMGA2*, FHL2*, CTGF*, NAGLU*, TAL1*, MDH2*, MRPL16*, C1QBP*, GATA1*, CXCL3*, MLEC, IRF8, DEPDC7, ZNF793, CCDC57, GNL3, APOE, RNF182, NCKAP5L

A

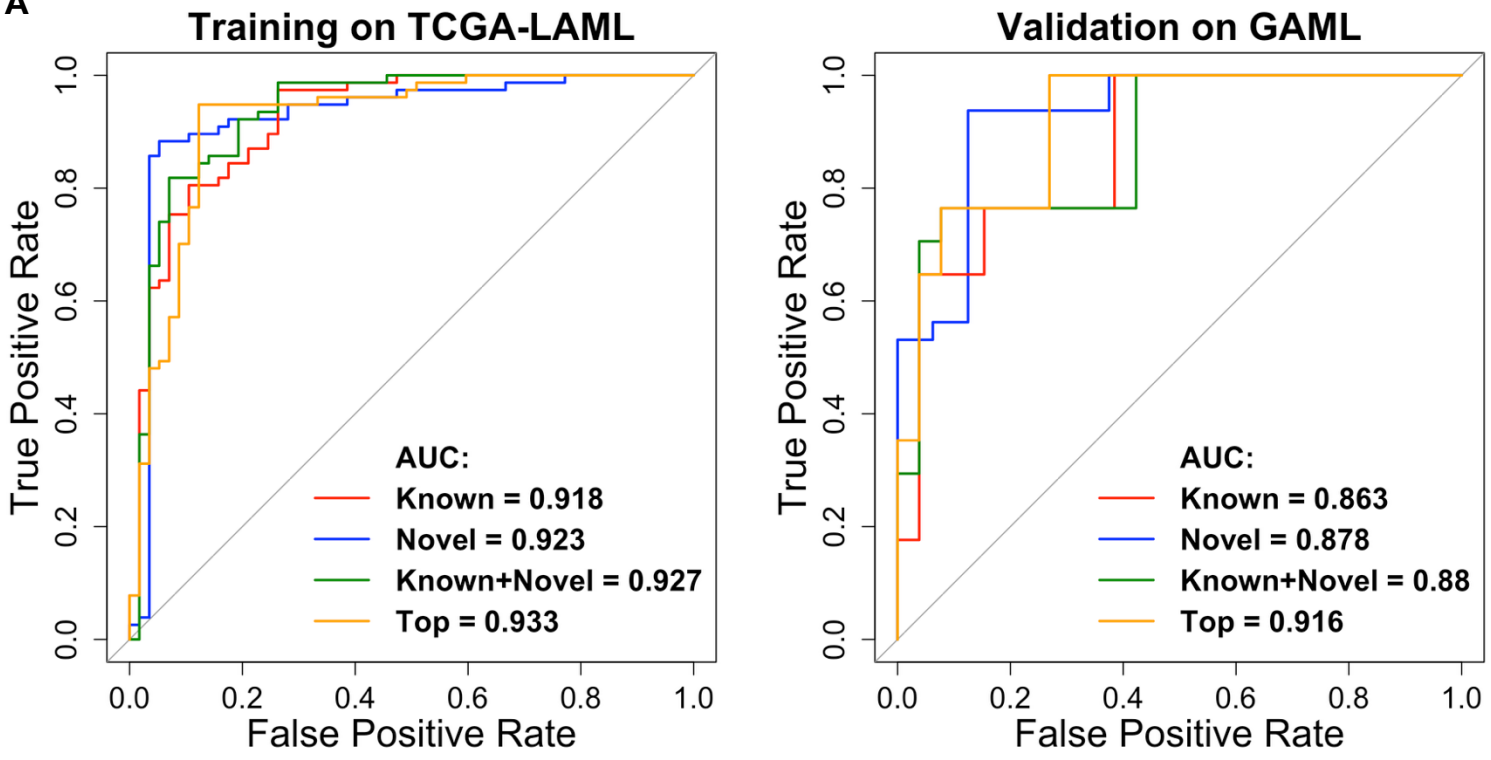

B

Genes	Accuracy	Precision	Recall	F1score	Specificity
Training on TCGA-LAML					
Known	0.84	0.87	0.74	0.8	0.92
Novel	0.87	0.9	0.77	0.83	0.93
All	0.9	0.89	0.91	0.9	0.92
Top	0.92	0.93	0.88	0.9	0.94
Validation on GAML					
Known	0.77	0.86	0.73	0.79	0.82
Novel	0.79	0.84	0.81	0.83	0.76
All	0.84	0.91	0.81	0.86	0.88
Top	0.86	0.89	0.89	0.89	0.82

C

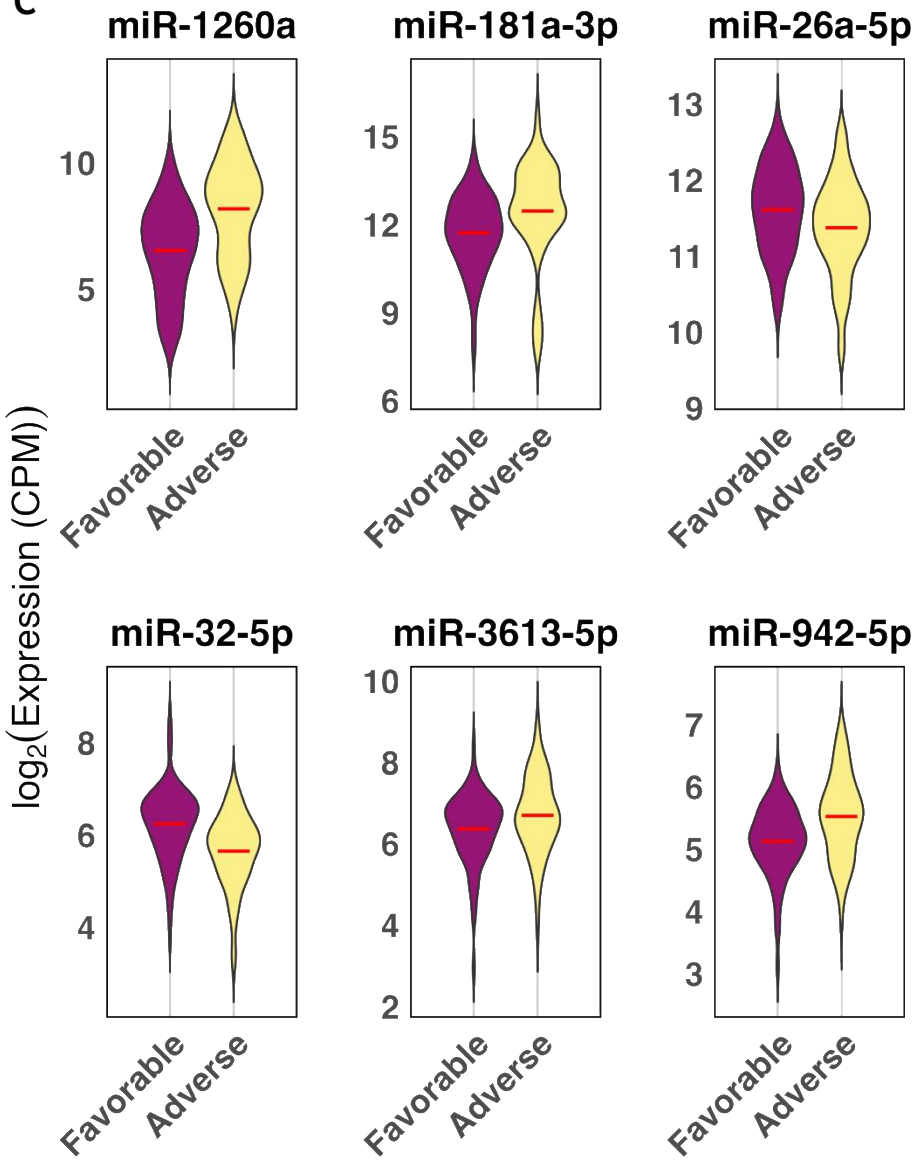

Top miRNAs: let-7b-3p*, miR-106a-5p*, miR-107*, miR-1260a, miR-1260b, miR-181a-3p*, miR-186-5p*, miR-197-3p, miR-203a-3p*, miR-26a-5p*, miR-32-5p, miR-335-5p*, miR-3613-5p, miR-450a-5p*, miR-942-5p, miR-7-5p*

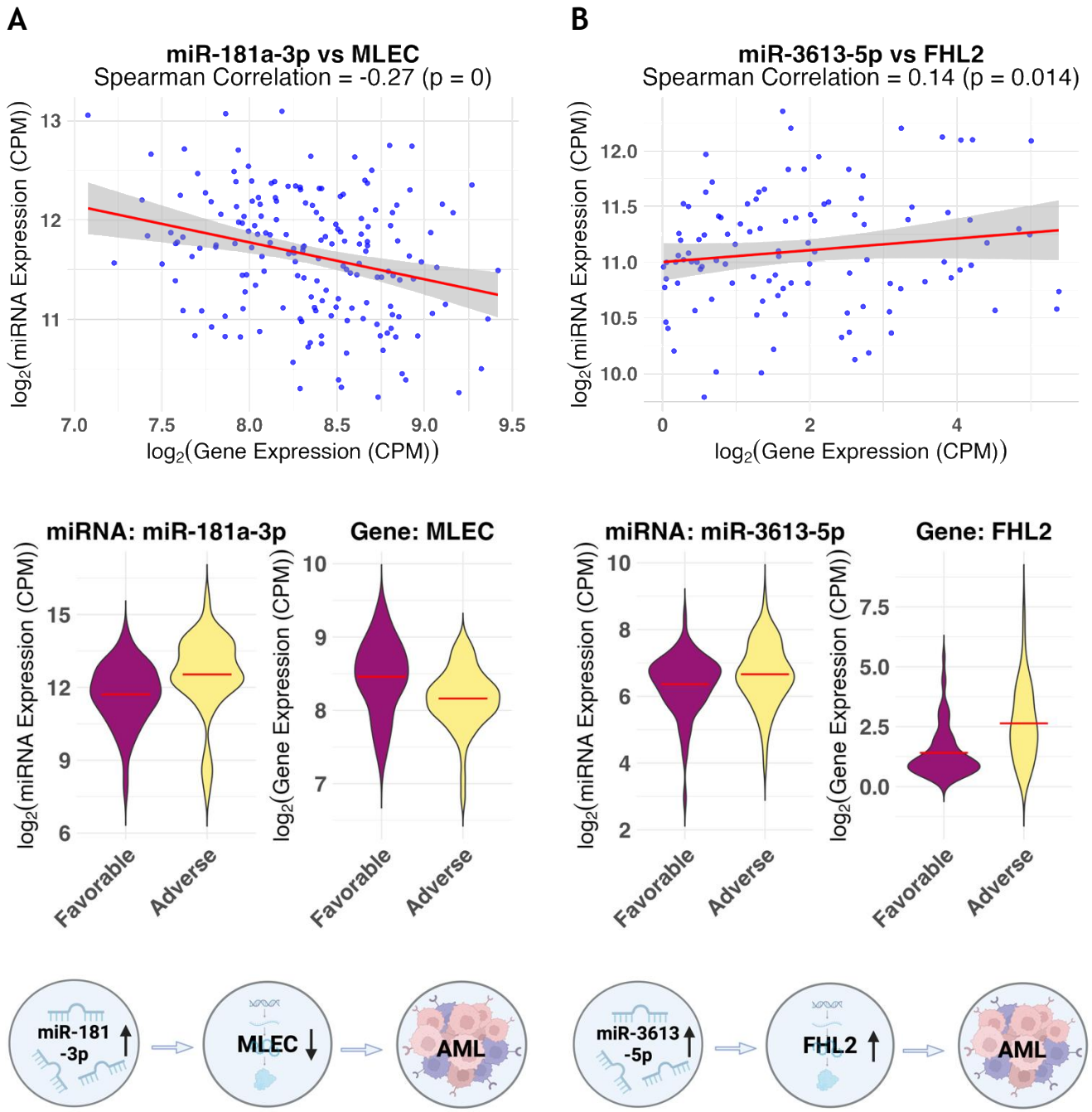

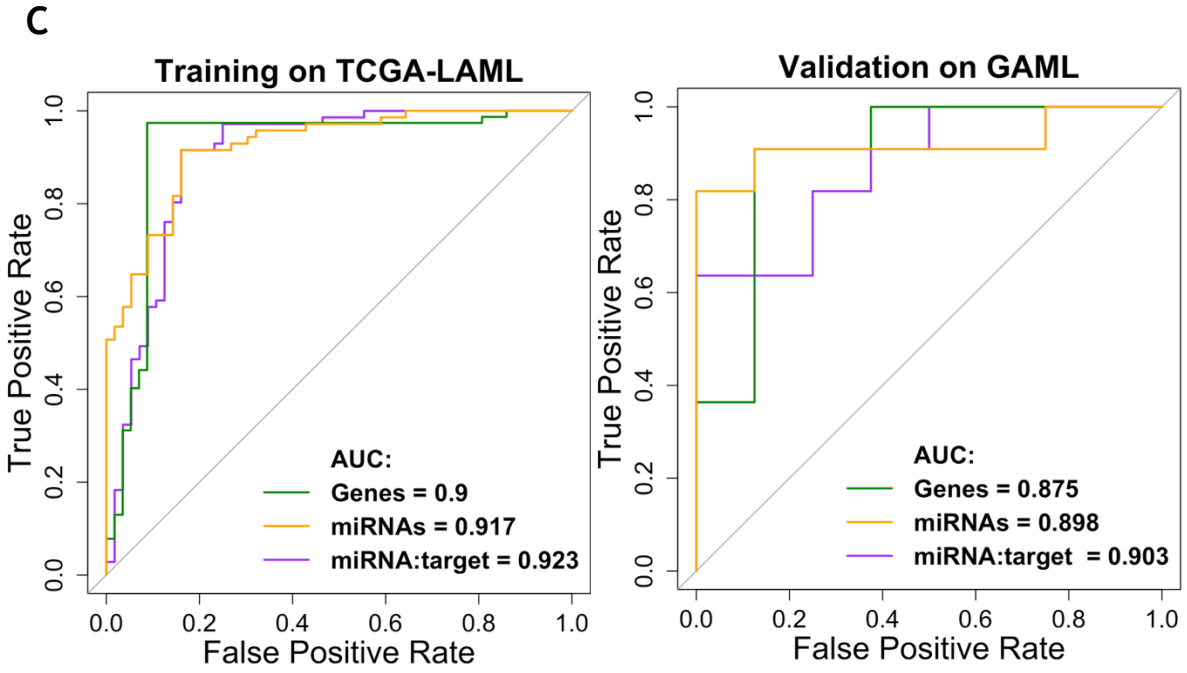

D

	Accuracy	Precision	Recall	F1score	Specificity
Training on TCGA-LAML					
Genes	0.88	0.89	0.84	0.86	0.92
miRNAs	0.9	0.91	0.86	0.88	0.93
Pairs	0.92	0.91	0.91	0.91	0.93
Validation on GAML					
Genes	0.84	0.78	0.88	0.82	0.82
miRNAs	0.84	0.86	0.75	0.8	0.91
Pairs	0.89	0.88	0.88	0.88	0.91

A

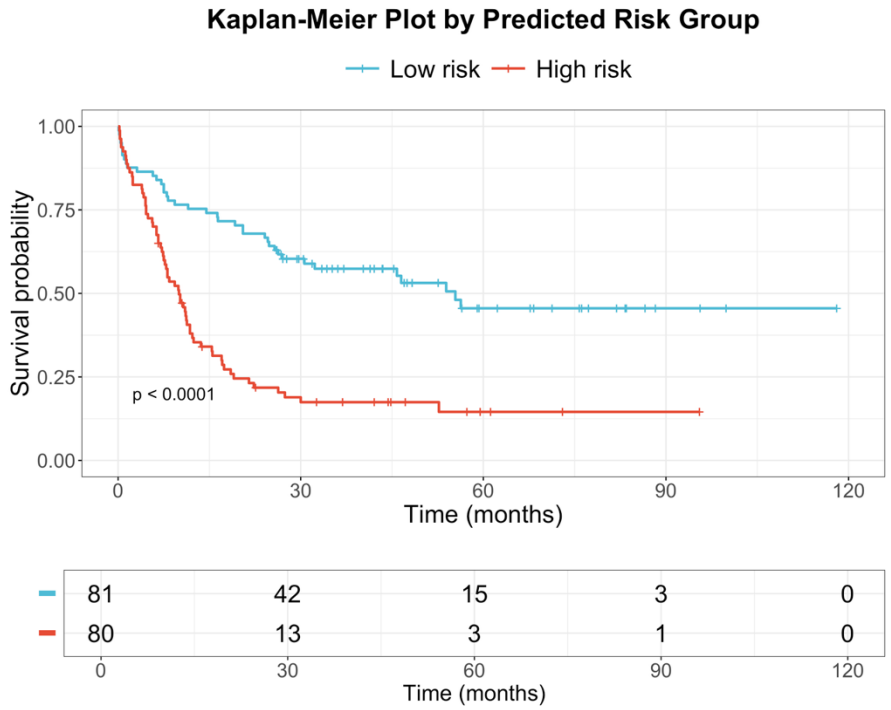

B

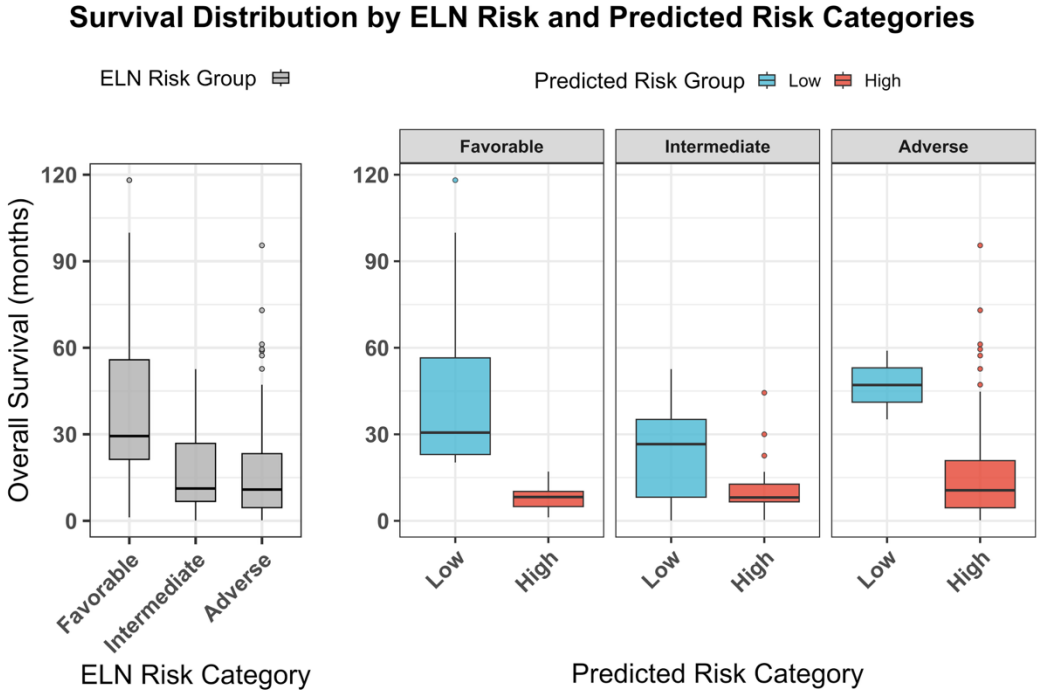

C

Threshold = 0.021	Favorable	Intermediate	Adverse
Low	65	14	2
High	6	20	54

D

Biomarkers	Beta	SE	BH- adjusted p-value	Oncogenic status
miR-1260a	-5.36×10^{-2}	6.55×10^{-3}	0.042	Unreported
miR-181a-3p*	5.85×10^{-1}	5.28×10^{-3}	0.041	Oncogene
miR-26a-5p*	-6.36×10^{-2}	9.52×10^{-3}	0.035	Tumor suppressor
miR-32-5p	-1.83×10^{-2}	2.76×10^{-3}	0.033	Unreported
miR-3613-5p	-3.79×10^{-2}	1.85×10^{-3}	0.008	Unreported
miR-942-5p	7.00×10^{-2}	2.54×10^{-3}	0.035	Unreported
MLEC	-2.95×10^{-2}	1.23×10^{-3}	0.032	Unreported
FHL2*	2.97×10^{-1}	4.78×10^{-3}	0.002	Oncogene
HMGA2*	1.33×10^{-2}	4.12×10^{-3}	0.029	Oncogene
MDH2*	3.63×10^{-2}	1.80×10^{-3}	0.035	Oncogene
APOE	-1.02×10^{-2}	6.14×10^{-4}	0.032	Unreported
DEPDC7	-5.23×10^{-2}	1.37×10^{-2}	0.019	Unreported
IRF8	7.35×10^{-3}	1.43×10^{-4}	0.035	Unreported
CCDC57	-2.03×10^{-3}	1.58×10^{-4}	0.036	Unreported

* Indicates known AML biomarkers